AD_____

Award Number: DAMD17-03-1-0501

TITLE: Brain's DNA Repair Response to Neurotoxicants

PRINCIPAL INVESTIGATOR: Juan Sanchez-Ramos, M.D., Ph.D.

CONTRACTING ORGANIZATION: South Florida University
Tampa, Florida 33620

REPORT DATE: July 2004

TYPE OF REPORT: Annual

PREPARED FOR: U.S. Army Medical Research and Materiel Command
Fort Detrick, Maryland 21702-5012

REPORT DOCUMENTATION PAGE

Form Approved
OMB No. 074-0188

1. AGENCY USE ONLY (Leave blank)	2. REPORT DATE	3. REPORT TYPE AND DATES COVERED
	July 2004	Annual (1 Jul 2003 - 30 Jun 2004)

4. TITLE AND SUBTITLE
Brain's DNA Repair Response to Neurotoxicants

5. FUNDING NUMBERS
DAMD17-03-1-0501

6. AUTHOR(S)
Juan Sanchez-Ramos, M.D., Ph.D.

7. PERFORMING ORGANIZATION NAME(S) AND ADDRESS(ES)
South Florida University
Tampa, Florida 33620

E-Mail: jsramos@hsc.usf.edu

8. PERFORMING ORGANIZATION REPORT NUMBER

9. SPONSORING / MONITORING AGENCY NAME(S) AND ADDRESS(ES)
U.S. Army Medical Research and Materiel Command
Fort Detrick, Maryland 21702-5012

11. SUPPLEMENTARY NOTES
Original contains color plates: All DTIC reproductions will be in black and white.

12a. DISTRIBUTION / AVAILABILITY STATEMENT
Approved for Public Release; Distribution Unlimited

12b. DISTRIBUTION CODE

13. ABSTRACT (Maximum 200 Words)
Parkinson's Disease (PD) is associated with death of dopaminergic (DA) neurons in the substantia nigra (SN) of the brain. Military personnel abroad are at a greater risk of exposure to pesticides and toxins which may selectively damage DA neurons in the SN and increase the probability of development of Parkinson's disease (PD) later in life. The toxins of interest are mitochondrial poisons that create a bioenergetic crisis and generate toxic oxyradicals which damage macromolecules, including DNA. We hypothesize that regulation macromolecules, including DNA. We hypothesize that regulation of the DNA repair response within certain neurons of the SN (the pars compacta) may be a critical determinant for their vulnerability to these neurotoxicants. We have measured regional differences in the brain's capacity to increase repair of oxidized DNA (indicated by oxyguanosine glycosylase (OGG1)activity) to three distinct chemical classes of neurotoxins (MPTP, two mycotoxins, and an organochloriine pesticide). At the end of the first year of the project, we have found that the temporal and spatial profile of OGG1 activity across brain regions elicted by each class of neurotoxicant is distinct and unique, but failure to maintain a vigorous increase in OGG1 and endogenous anti-oxidant activity in specific brain loci appears to be a shared mechanism leading to neuronal injury in that region.

14. SUBJECT TERMS
DNA damage, DNA repair, brain, neurotoxicants, mycotoxins

15. NUMBER OF PAGES
32

16. PRICE CODE

17. SECURITY CLASSIFICATION OF REPORT	18. SECURITY CLASSIFICATION OF THIS PAGE	19. SECURITY CLASSIFICATION OF ABSTRACT	20. LIMITATION OF ABSTRACT
Unclassified	Unclassified	Unclassified	Unlimited

Table of Contents

INTRODUCTION

Parkinson's Disease (PD) is associated with death of dopaminergic (DA) neurons in the substantia nigra (SN) of the brain (3-5). Military personnel abroad are at a greater risk of exposure to pesticides and toxins (1) some of which may selectively damage DA neurons in the SN and increase the probability of development of Parkinson's disease (PD) later in life. The toxins of interest are mitochondrial poisons that create a bioenergetic crisis and generate toxic oxyradicals which damage macromolecules, including DNA. We hypothesize that the DNA repair response within certain neurons of the SN (the pars compacta) may be a critical determinant for their vulnerability to these neurotoxicants. The technical objectives were to measure regional and cellular differences in the brain's DNA repair response to three neurotoxins known to interfere with mitochondrial function (the mycotoxin ochratoxin-A; the pesticide dieldrin, and the classic dopaminergic neurotixn, MPTP). An improved understanding of the DNA repair response to neurotoxicants and development of methods to enhance DNA repair will form the basis for potential preventive measures against the effects of military threat agents and military operational hazards, and also lead to treatment interventions for Parkinson's disease

BODY

TASK 1. MEASUREMENT OF REGIONAL DIFFERENCES IN OXIDATIVE DNA DAMAGE AND DNA REPAIR RESPONSES ELICITED BY MYCOTOXINS (OCHRATOXIN-A, RUBRATOXIN), ORGANOCHLORINE PESTICIDES (DIELDRIN) AND BY THE CLASSICAL DA NEUROTOXIN, MPTP. (MONTHS 1-18):

a) Administer single doses (over a range of doses) of each neurotoxin (ochratoxin A, rubratoxin, dieldrin and MPTP) into separate groups of mice; euthanize groups of mice at 6, 24 and 72 hrs; dissect brain regions on ice and freeze until assays are performed (Month 1-3)
b) Measure oxo^{8}dG (as index of oxidative DNA damage) in all tissue samples (Month 3)
c) Determine enzymatic activities, mRNA and protein expression of OGG1, Ref-1, PARP-1 and β-polymerase (Months 4-7)
d) Measure effects on striatal dopamine and homovanillic acid and on the number of DA neurons and apoptotic profiles in substantia nigra (SN) (Months 8-10);
e) Determine and analyze the dose-response functions for each parameter of the DNA repair response for each neurotoxicant; analyze quantitative and temporal relationships between degree of DNA damage and DNA repair change over time (6, 24 and 72hrs) (Months 11-12)

Effects of Rubratoxin (RB)

We have completed an analysis of the results of RB administration on DNA damage and repair in brain. The published report can be found in *Gene Expression* (6) (See Appendix for reprint p 13). We present here a brief summary of the findings. Parameters of oxidative DNA damage and repair, lipid peroxidation and superoxide dismutase (SOD) activity were measured across 6 mouse brain regions 24 hrs after administration of a single dose of RB. This dose was chosen on the basis of a dose-toxicity curve that produced minimal hepatotoxicity and did not result in gross damage to brain. The salient findings were as

follows: Lipid peroxidation was paradoxically and significantly decreased in three brain regions, hippocampus (H), midbrain (MB) and pons/medulla(PM). Unexpectedly, oxidative DNA damage (indicated by 8-oxodG levels) did not increase in any brain region, but instead showed a slight decrease in all regions with a statistically significant decrease in the PM. Concomitant with decreased indices of oxidative macromolecular damage, SOD activity was increased significantly in all brain regions. Similarly, oxyguanosine glycosylase activity (OGG1) was increased in three brain regions CB, CP and CX in RB-treated mice compared to vehicle-treated controls. The RB-enhanced OGG1 activity was not due to increased OGG1 protein expression, but was a result of enhanced catalytic activity. In conclusion, specific brain regions responded to an acute dose of RB by significantly increasing endogenous anti-oxidant activity (SOD) and DNA repair (OGG1) activities. This was associated with a net decrease in measures of lipid peroxidation in 3 brain regions and a significant decrease in oxidative DNA damage in hippocampus.

The mechanisms underlying the vulnerability of the brain to different neurotoxicants is complex, but we hypothesize that the capacity to regulate and repair oxidative DNA damage, and to modulate endogenous anti-oxidant enzymes, are important determinants of a brain region's susceptibility to RB. In the present study with RB, which focused on a single time point 24 hrs after injection with RB, it was not possible to determine the earliest signals for triggering and amplifying SOD and OGG1 activities. We imposed the limitation of a single time point for this study, since we were interested in the differential response across brain regions. The robust anti-oxidant response and enhanced OGG1 catalytic activity in some regions resulted in much lower levels of oxidized base in those brain regions, providing a clue as to the selective vulnerability of specific neuronal populations located in those regions.

Since completeing that study, we have learned that rubratoxin is no longer available for purchase commercially (Sigma has discontinued its production and sale). Hence we were not able to perform a time course study with rubratoxin. Ochratoxin A is still available and we were able to perform the studies described below.

Ochratoxin A (OTA)

Effects on DA levels. Before initiating studies on the brain's DNA repair response to OTA, a dose response study of the effects of OTA on DA levels in midbrain and striatum was performed. OTA administration resulted in a dose-dependent decrease in striatal (caudate/putamen) DA. (Figure 1). An EC50 of 3.6 mg/kg was calculated and subsequent studies utilized a test dose of 4 mg/kg i.p.

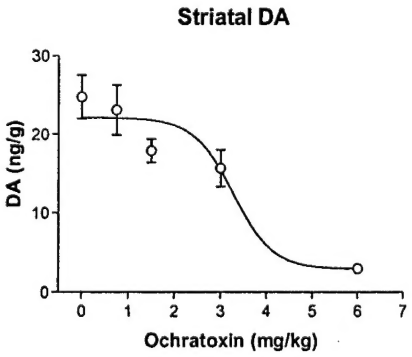

Figure 1 Effects of OTA on striatal DA

Effects of OTA (4 mg/kg ip) on regional brain OGG1 activity over time

In all brain regions the initial response at 6 hrs was a decrease in OGG1 activity, followed by a tendency to recover towards control levels. In cerebellum, midbrain and pons/medulla, there was a significant recovery towards approximately control levels by 72 hrs. In hippocampus, cerebral cortex and caudate/putamen, the OGG1 activities recovered to some extent, but remained significantly below control levels.

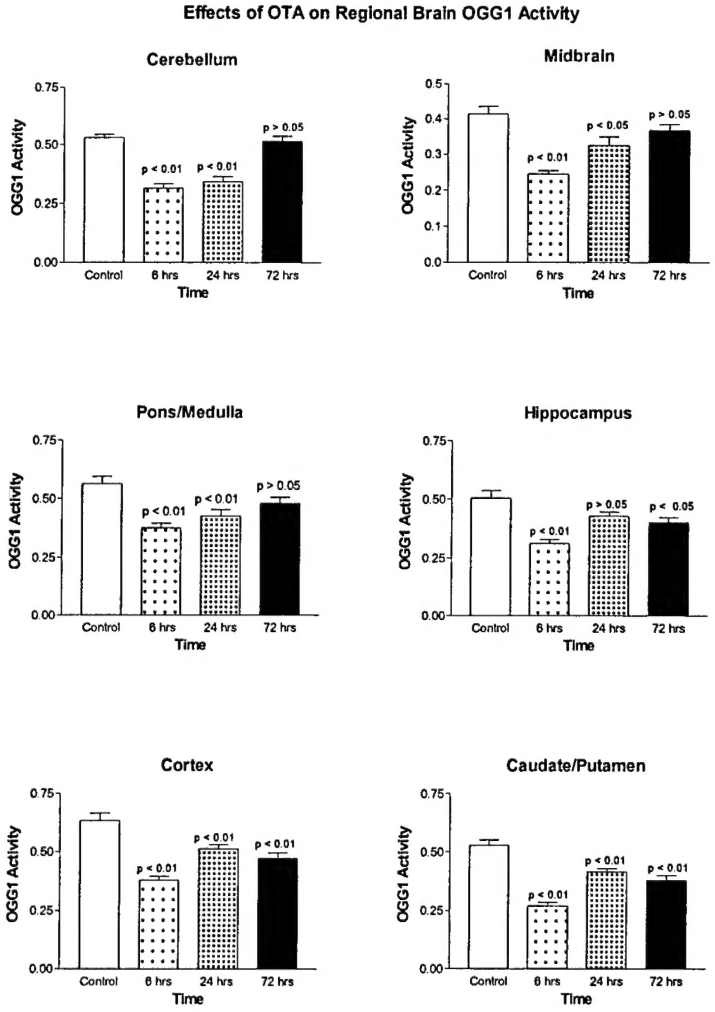

Figure 2

Time-course of effects of an acute dose of OTA on OGG1 activities. Two-way ANOVA (using unweighted means analysis) revealed that time accounted for 50% of the variance and brain region accounted for 23% of variance (both were significant at p< 0.0001). An interaction between time and brain region accounted for 8% of variance (p=0.008).One way analysis of variance for each brain region over time revealed that the means were significantly different with a p < 0.001. Post-test analysis included Dunnett's Multiple Comparison Test which compared mean OGG1 activity at each time period to appropriate controls value for each brain region.

Effects of MPTP

A single dose of MPTP 20 mg/kg was chosen that produces a partial lesion of the nigro-striatal DA system. The time-course of effects of this dose on DA levels in the two DA systems (the motor nigro-striatal system and the VTA to N. accumbens system) is shown in Figure 3. Under control conditions the highest concentrations of DA were in the CP and ventral striatum (N. accumbens). Following a single dose of MPTP, levels of DA decreased significantly and remained below control levels for 72 hours in all regions. The DA level in the CP was reduced to its nadir (26% of control levels) at 24 hrs and the SN reached its lowest levels (15% of control) at 48 hrs. The VTA was reduced to its nadir (23% of control) at 72 hrs and the N. Acb. reached its lowest level (52% of control) at 24 hrs. The DA levels in N. Acb. appeared to be recovering slightly by 72 hrs. These results are consistent with other reports that show that the VTA and N. accumbens are less susceptible to MPTP than the nigro-striatal system.

Concomitant with the decreasing DA levels in the nigro-striatal system, the endogenous anti-oxidant SOD activity increased significantly over time reaching a peak at 48 hrs and then declined below control level at 72 hrs. In the VTA and N. Acb, the SOD also increased and peaked at 48 hrs but then declined below control levels at 72 hrs (Figure 3).

Repair of oxidized DNA damage also increased with time in the nigro-striatal DA system, reaching a peak at 48 hrs and declining, but not dipping below control levels, at 72 hrs. In particular, OGG1 activity in S. nigra returned to near control levels by 72 hrs.

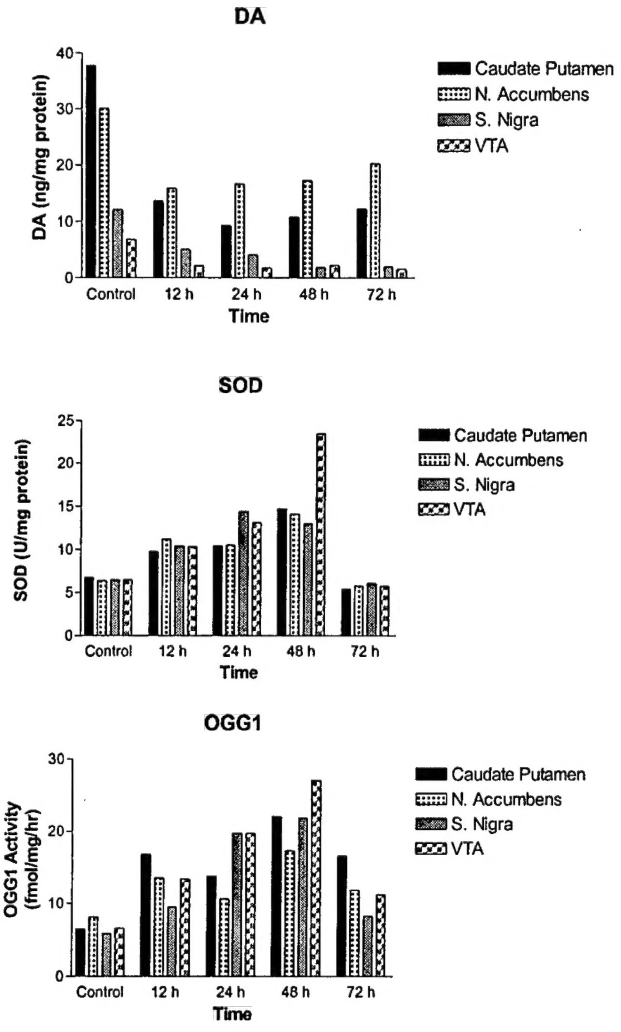

Figure 3.

Top Panel Mean DA levels in 4 micro-dissected regions following an acute does of MPTP. SEM bars are less than 15% of the mean and are not shown. DA concentrations at all time points were significantly different than control levels for each region ($p < 0.05$).

Middle Panel: Effects on SOD Activity. SOD in all regons increase significantly ($p < 0.05$) at 12, 24 and 48 hrs. At 72 hrs the levels have declined to levels below control SOD activity in all regions.

Lower Panel Effects on OGG1 Activity. OGG1 activity increased significantly at 12, 24, 48 hrs in all regions. At 72 hrs, levels of OGG1 declined in all regions and nearly returned to control levels in S. nigra.

OGG1 response to MPTP in other brain regions

Although MPTP is known to be selectively toxic for dopaminergic neurons, it was of interest to see a widespread and sustained anti-oxidative and DNA repair response in brain loci that escape permanent MPTP injury. We performed micro-punches of 44 regions of mouse brain (See Appendix Table A-1, and A-2 for descriptive details). For each sample of tissue (1 mm X 1mm X 1 mm), OGG1 activity and SOD activity was measured (See Appendix, Tables A-3 and A-4 for summary data from all brain regions and time points).

Regions such as those found in cerebellum, hippocampus and most loci of the cerebral cortex (with the exception of the lateral orbital cortex) exhibited a sustained increase of OGG1 activity through 72 hrs (Figures 4-7). In the pons/medulla, the locus ceruleus and the motor nucleus of the Vth cranial nerve showed a sustained increase in OGG1 activity up to 72 hrs (Figure 4). The locus ceruleus, like the s. nigra and striatum, was clearly impacted by MPTP as evidenced by decreased tyrosine hydroxylase (TH) immunoreactivity in those structures (See Appendix p19 Fig A-1). Unlike the s. nigra and striatum (and reticular tegmental nucleus of the pons), the locus coeruleus was able to maintain repair of oxidized DNA damage at a high level up through 72 hours.

Figure 4

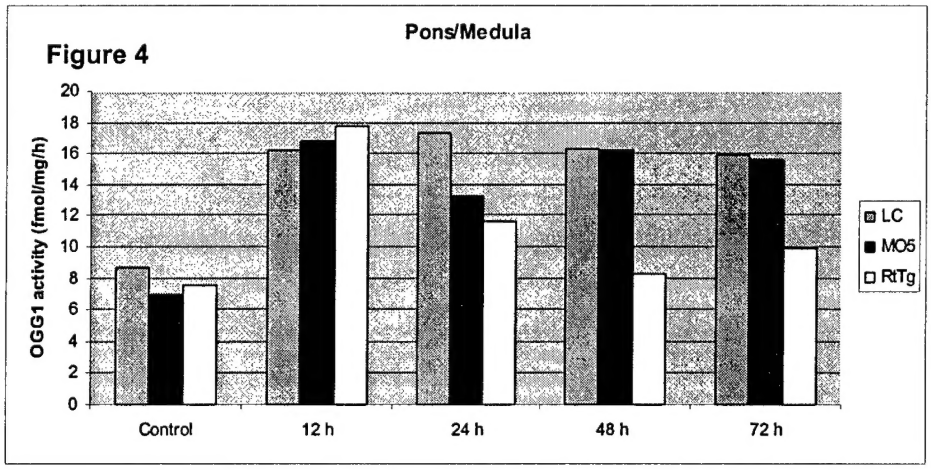

	Control	12 h	24 h	48 h	72 h
LC (locus ceruleus)	8.683835	16.23705	17.30939	16.29762	15.95088
MO5 (motor nucleus of V cranial nerve)	6.971875	16.86961	13.25608	16.2752	15.62792
RtTg (reticulo-tegmental nucleus of pons)	7.556655	17.74976	11.62405	8.223339	9.867094

Figure 5

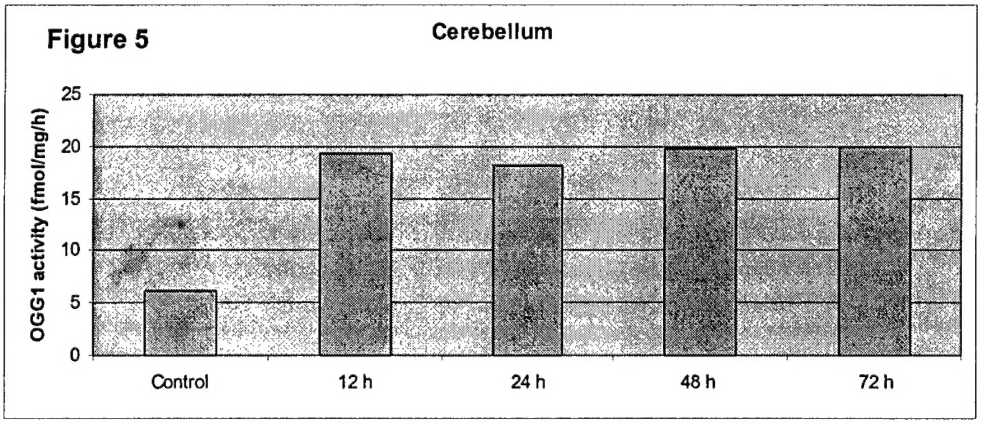

Figure 6

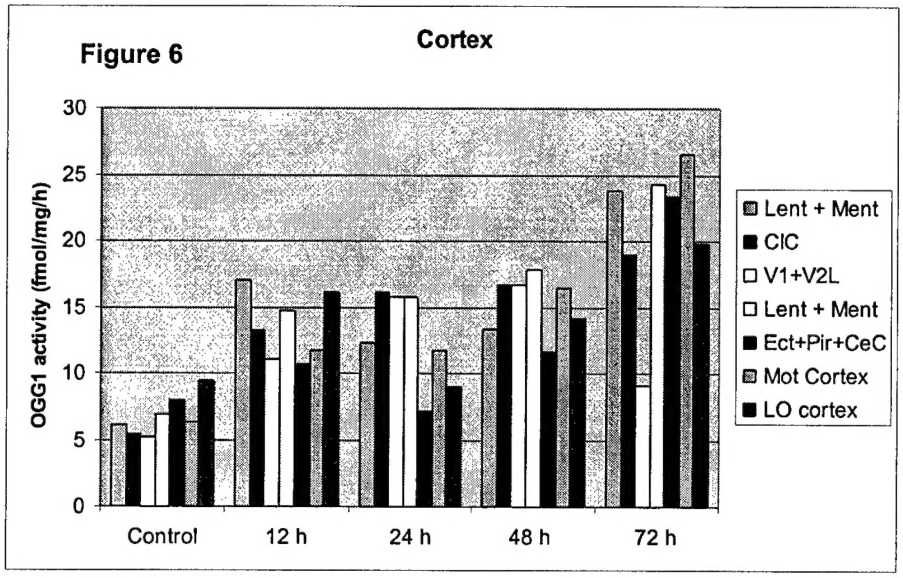

	Control	12 h	24 h	48 h	72 h
LEnt	6.112702	17.05585	12.25431	13.3058	23.77718
CIC	5.445382	13.18197	16.11283	16.65993	18.91756
VIB	5.193619	11.0885	15.7544	16.6398	9.112203
cortex	6.854752	14.68313	15.75846	17.81964	24.25495
Cortex S2	7.968963	10.66728	7.163959	11.63909	23.36639
Mot Cortex	6.363964	11.73458	11.76573	16.46481	26.50132
LO cortex	9.410617	16.13409	8.988234	14.08366	19.78213

Figure 7

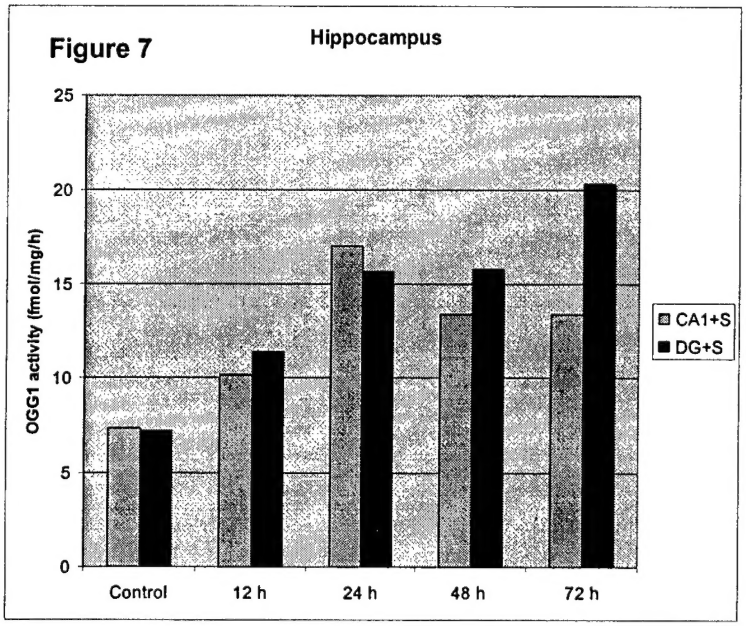

	Control	12 h	24 h	48 h	72 h
CA1+S	7.334379	10.14105	17.02738	13.37833	13.36933
DG+S	7.258228	11.35563	15.68427	15.81669	20.31449

Immuno-histochemical analysis

Immunoreactivity for TH and the dopamine transporter (DAT) were markedly decreased in both caudate/putamen and s. nigra 72 hrs after a single dose of MPTP (See Appendix Fig. A-2). Assessment of apoptosis using TUNEL staining revealed a significant number of apoptotic nuclei in the s. nigra at 72 hours. Apoptotic nuclei were rare under control conditions or at 12, 24 or 48 hrs (See Appendix p 20 Figs A3-4). Concomitant with the marked degree of apoptosis that became evident in s. nigra at 72 hrs, there was a large drop-off of anti-oxidative and DNA repair activity in this locus. Apparently the oxidative challenge elicited by MPTP was unable to be checked and maintained by the vigorous increase in SOD and OGG1 activities in the s. nigra.

The DNA repair response across brain regions to the mycotoxin, OTA, was quite different from that elicited by MPTP. OTA initially inhibited OGG1 activity in all brain regions, but by 72 hrs the response tended to recover towards normal, with the exception of the striatum, hippocampus and cortex, where OGG1 remained significantly lower than control levels. From this profile of OGG1 activation, it can be inferred that the striatum, hippocampus and cortical regions are most likely to suffer permanent injury and neuronal apoptosis following acute administration of OTA.

Effects of Dieldrin (30 mg/kg i.p.)

Effects on DA levels Dieldrin administration resulted in an initial rapid decrease in striatal DA levels at 6 hrs followed by an increase in DA concentrations and an increased turnover (ratio of HVA to DA) by 72 hrs (See Figure 8). A similar pattern was observed in the midbrain (data not shown).

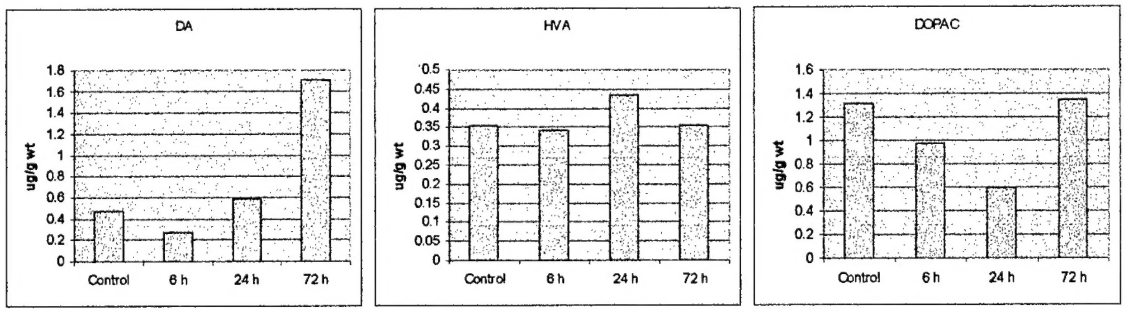

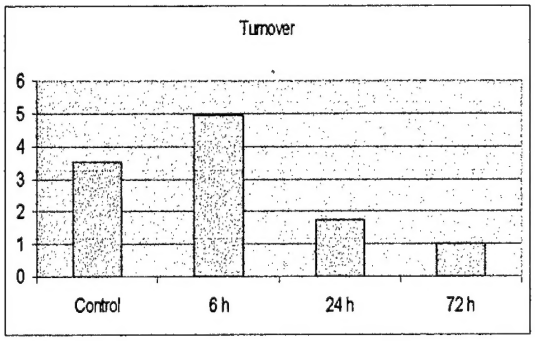

Figure 8 Effects of Dieldrin (30 m/kg) on Striatal DA, HVA , DOPAC and DA turnover (HVA+DOPAC/DA) at 6, 24 and 72 hrs.

Effects on OGG1 Following a single i.p. injection of 30 mg/kg, dieldrin triggered a sustained and statistically significant increase in OGG1 activity across the six regions of brain (Figure 9). Most interestingly, the OGG1 response was maintained in the striatum, a region in which dieldrin significantly decreased DA levels within 6 hrs but which over the subsequent 72 hrs resulted in significantly increased DA levels. DA turnover (the ratio of DA metabolites to DA levels) was initially increased (at 6 hrs) but then significantly decreased at 24 and 72 hrs. Although the effects of dieldrin in s. nigra (and VTA) have not yet been completed, this profile of response is very different from that of MPTP. The data so far have revealed that dieldrin elicits a generalized oxidative stress that triggers OGG1 activity across all brain regions for up to 72 hours.

CONTROL				6 HOURS		
#	Mean	SEM	N	Mean	SEM	M
cb	2.936841	0.324848	6	6.883521	0.529305	5
mb	2.06068	0.259453	6	7.762494	0.69326	5
pm	2.014374	0.244405	6	7.147105	0.749354	5
hp	2.868504	0.33947	6	8.369375	0.878907	5
cp	2.086568	0.272153	6	7.909312	0.810995	5
cx	2.415506	0.357937	6	6.109506	0.407693	5
CONTROL				24 HOURS		
#	Mean	SEM	N	Mean	SEM	M
cb	2.936841	0.324848	6	5.895929	0.800826	5
mb	2.06068	0.259453	6	6.060747	0.717432	5
pm	2.014374	0.244405	6	5.144618	0.483894	5
hp	2.868504	0.33947	6	5.650633	0.273939	5
cp	2.086568	0.272153	6	5.806164	0.655318	5
cx	2.415506	0.357937	6	4.91238	0.473463	5
CONTROL				72 HOURS		
#	Mean	SEM	N	Mean	SEM	M
cb	2.936841	0.324848	6	7.536823	0.872216	5
mb	2.06068	0.259453	6	10.29313	1.196714	5
pm	2.014374	0.244405	6	8.785135	1.00328	5
hp	2.868504	0.33947	6	9.801442	0.963987	5
cp	2.086568	0.272153	6	8.781804	0.451351	5
cx	2.415506	0.357937	6	7.310648	0.282688	5

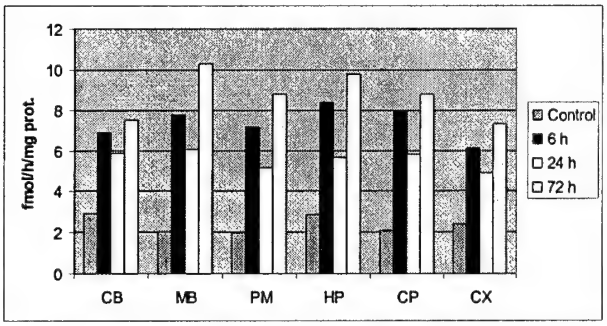

Figure 9 Effects of dieldrin (30 mg/kg) i.p. on OGG1 activity across six brain regions at 6, 24 and 72 hrs. The table to the left shows the summary data. The mean OGG1 activites were significantly elevated ($p < 0.5$) compared to control at all time points in each brain region.

KEY RESEARCH ACCOMPLISHMENTS

1) The effects of two mycotoxins (ochratoxin-A and rubratoxin-B), and an organochlorine pesticide (dieldrin) on the capacity of brain to repair oxidative damage to DNA was studied and compared to a well-known neurotoxicant (MPTP) that selectively injures the nigro-striatal DA system.
2) The acute effects of ochratoxin, MPTP and Dieldrin on DA and its metabolites in the nigro-striatal DA system was measured.

3) The regulation of the DNA repair enzyme (OGG1) across brain regions was studied for each of the toxicants.
4) A spatial (neuroanatomical) and temporal mapping of the brains DNA repair and anti-oxidative response to the neurotoxicants was produced.

REPORTABLE OUTCOMES

We were able to generate a temporal and spatial profile of OGG1 and SOD activity elicited by an acute challenge with three distinct classes of neurotoxicants. Even though each of the three classes of neurotoxicants studied here is known to interfere with mitochondrial function, the OGG1 activity profile across brain regions has revealed interesting differences in the vulnerability of specific regions of brain to each class of toxicant. Ochratoxin-A produced an initial depression of OGG1 activity in six brain regions, but with time there was an increase in OGG1 in all regions except for a) hippocampus, b) caudate/putamen and c) cerebral cortex. These are the brain regions that are most affected following an episode of hypoxia/ischemia (eg hippocampus, cerebral cortex and globus pallidus) (2). From this profile of OGG1 reactivity, it may be inferred that OTA toxicity mimics the effects of global hypoxia on brain. By contrast, an acute challenge with MPTP resulted in an increase of OGG1 activity in all brain regions within the first 6 hrs. The augmented OGG1 activity was maintained up through 48hr. This response was completely unexpected because MPTP is considered to be a selective nigro-striatal dopamergic neurotoxin and such a wide-spread activation of anti-oxidant and OGG1 activity had never been reported. However, by 72 hrs, there was a significant decrease of repair capacity, most notably in the nigro-striatal DA system. Even though the locus coeruleus was affected by MPTP, as evidenced by a decrease in TH immunoreactivity similar to that observed in s. nigra and striatum, the OGG1 activity in that neuronal population remained at a high level through 72 hours and was consistent with its resistance to MPTP neurotoxicity. In the s. nigra, the big drop in SOD and OGG1 activity at 72 hours was associated with a significant increase in the number of apoptotic cells in that nucleus. Dieldrin's profile of OGG1 activation was distinct from those of MPTP and OTA. Dieldrin triggered a generalized OGG1 response that remained elevated through 72 hrs. There was no drop-off of activity in the striatum or other brain regions. To summarize, the temporal and spatial profile of MPTP-triggered DNA repair and anti-oxidant activity at 72 hrs was consistent with the well known localized toxicity for the nigro-striatal DA system. The very distinct profile of the DNA repair and anti-oxidant activity triggered by OTA suggests that this mitochondrial toxicant produces effects similar to a global hypoxic episode. Finally, the response to dieldrin revealed that all brain regions were able maintain the DNA repair response for 72 hrs despite an alteration of DA turnover in the striatum, and apparently none of the 6 brain regions was selectively vulnerable to this agent. Of course a more detailed neuroanatomical analysis of the diedlrin response (in particular the s. nigra compacta and VTA) remains to be completed before arriving at any conclusions with regard to this neurotoxicant.

CONCLUSIONS

The findings reported here in this first year's progress report support the hypothesis that the DNA repair response plays a role in determining the vulnerability of specific brain regions to three distinct classes of neurotoxicants that share a common mechanism of mitochondrial toxicity. Mapping the spatial and temporal profiles of DNA repair and anti-oxidative responses to neurotoxicants will be helpful in understanding the pathogenesis and neurological consequences of toxicant-induced injury to the central nervous system. However, it is still possible that differences in the distribution of the mycotoxins across brain regions are important in determining regional vulnerabilities for that toxin. To address this important concern, we will modify the proposal for the immediate next period to include measurement of the distribution of ochractoxin in each micro-dissected brain region followed by a correlation with OGG1 and anti-oxidant activities across the set of brain loci. In the case of MPTP, it is well known that the concentration of MPP+ (the active metabolite of MPTP) is highest in dopaminergic neurons, thereby accounting for its selective toxicity to neurons of the nigro-striatal system. However, it is still not clear why the DA neurons of the VTA are less vulnerable to MPTP than the DA of the S. nigra compacta. Towards the end of year two, we will apply laser capture microdissection technique to collect two sets of dopaminergic neurons from midbrain: s.nigra compacta neurons and ventral tegmental area (VTA) DA neurons. Though both sets of neurons appear to be equally exposed to MPP+, the VTA neurons have been shown to be less vulnerable than s. nigra compacta neurons to both MPTP and to degeneration in idiopathic PD. If we can demonstrate VTA neurons can upregulate a series of DNA repair genes as well as anti-oxidant genes (using real-time RT PCR) to a greater extent than s. nigra compacta, then the hypothesis will have firmer ground. On this basis, it then becomes reasonable to screen for neuroprotective agents that pre-condition and up-regulate the DNA repair and anti-oxidant response to a level sufficient to neutralize the deleterious pro-oxidant molecular events triggered by a subsequent exposure to a mitochondrial neurotoxicant.

REFERENCES

1. Bennett, J. W., and Klich, M. 2003. Mycotoxins. *Clin Microbiol Rev* **16:** 497-516.
2. Cervos-Navarro, J., and Diemer, N. H. 1991. Selective vulnerability in brain hypoxia. *Crit Rev Neurobiol* **6:** 149-182.
3. Hornykiewicz, O. 1982. *Brain neurotransmitter changes in Parkinson's disease*. Butterworth, Boston.
4. McGeer, P. L., McGeer, E. G., and Suuki, J. S. 1977. Aging and extrapyramidal function. *Arch Neurol* **34:** 33-35.
5. Reiderer, P., and Wuketic, S. 1976. Time course of nigrostriatal degeneration in Parkinson's disease. *J Neural Trans* **3:** 277-301.
6. Sava, V., Mosquera, D., Song, S., Stedeford, T., Calero, K., Cardozo-Pelaez, F., Harbison, R., and Sanchez-Ramos, J. 2004. Rubratoxin B elicits antioxidative and DNA repair responses in mouse brain. *Gene Expr* **11:** 211-219.

APPENDIX
(Contents)

Table A-1. The representative microphotographs of brain slices of 1 mm thickness obtained after micro-punch sampling under light microscope at a magnification x 1.5

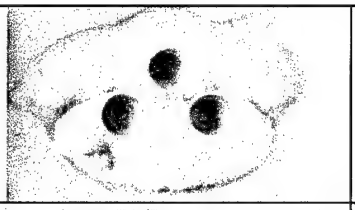	Bregma –5.68 ± 0.5 mm
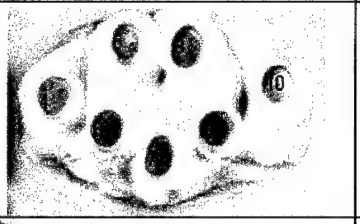	Bregma –4.86 ± 0.5 mm
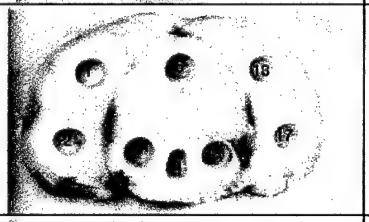	Bregma –3.88 ± 0.5 mm
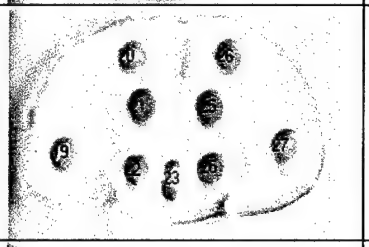	Bregma –2.92 ± 0.5 mm
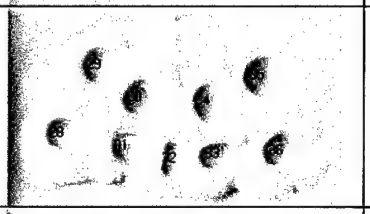	Bregma –1.46 ± 0.5 mm
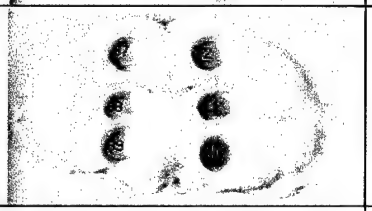	Bregma 1.42 ± 0.5 mm
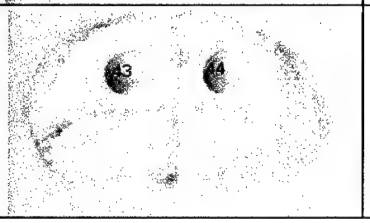	Bregma 2.80 ± 0.5 mm

Table A-2. Sampling of mouse brain tissue using micro-punch biopsy technique (regions were identified and named using the Atlas of Mouse Brain (Paxinos and Franklin, Academic Press, 2001).

Punch Position	Anatomical names	Abbreviations
1	locus coeruleus + medial parabrachial nu	LC+MPB
2	cerebellum lobules (2&3)	CB lob
3	locus coeruleus + medial parabrachial nu	LC+MPB
4	lateral entorhinal + medial entorhinal cortex	LEnt + MEnt
5	inferior colliculus + external & dorsal cortex	CIC + ECIC + DCIC
6	motor trigeminal nu	MO5
7	reticulotegmental nu pons	RtTg
8	motor trigeminal nu	MO5
9	inferior colliculus + external & dorsal cortex	CIC + ECIC + DCIC
10	lateral entorhinal + medial entorhinal cortex	LEnt + MEnt
11	Primary and secondary visual cortex	V1 + V2L
12	CA1 and subiculum of hippocampus	CA1 + S
13	substantia nigra (compact & reticular parts)	SNC + SNR
14	ventral tegmental area + interpeduncular nucleus	VTA + IPC + IPR
15	dorsomed periaqueductal grey	DMPAG
16	substantia nigra (compact & reticular parts)	SNC + SNR
17	CA1 and subiculum of hippocampus	CA1 + S
18	Primary and secondary visual cortex	V1 + V2L
19	Lateral entorhinal cortex	LEnt
20	Dentate gyrus and subiculum of hippocampus	DG + S
21	Post thalamic nu group + posterior intralaminar thalamic nu + med geniculate nu, med & ventral	PoT + PIL + MGV + MGM
22	substantia nigra	SN
23	supramammillary nu	sumx + SuM
24	substantia nigra	SN
25	Post thalamic nu group + posterior intralaminar thalamic nu + med geniculate nu, med & ventral	PoT + PIL + MGV + MGM
26	Dentate gyrus and subiculum of hippocampus	DG + S
27	Lateral entorhinal cortex	LEnt
28	entorhinal cortex, piriform cortex, basolateral amygdala	Ect + Pir + Blp
29	dentate gyrus	DG
30	posterior thalamic nu	PO + VPM
31	ventromedial thalamic nu	VM + ZID + ZIV
32	hypothalamic area	DMV + DMD + PH
33	ventromedial thalamic nu	VM + ZID + ZIV
34	posterior thalamic nu group	PO + VMP
35	dentate gyrus	DG
36	entorhinal cortex, piriform cortex, central amygdala	Ect + Pir + CeC
37	primary & secondary motor cortex	M1 + M2
38	caudatum putamen (striatum)	Cpu
39	accumbens nu, core + anterior commissure, anterior part	AcbC + aca
40	accumbens nu, core + anterior commissure, anterior part	AcbC + aca
41	caudatum putamen (striatum)	Cpu
42	primary & secondary motor cortex	M1 + M2
43	lateral orbital cortex	LO
44	lateral orbital cortex	LO

Table A-3. Distribution of SOD activity across the mouse brain during exposure to MPTP (20 mg/kg, ip)

Punch Position	Control	12 hours	24 hours	48 hours	72 hours
1	6.64±0.67	12.93±0.88*	13.36±1.72*	6.81±0.31	9.9±0.25*
2	6.54±0.42	9.41±1.07*	11.85±2.22*	6.13±0.34	10.57±0.86*
3	7.08±0.47	11.99±1.21*	12.57±2.45	9±0.24*	11.26±1.23*
4	6.76±0.43	12.36±1.81*	8.94±0.67*	6.17±0.20	15.77±0.36*
5	6.85±0.39	12.21±1.75*	14.59±1.75*	6.02±0.37	10.21±0.46*
6	6.62±0.45	9.47±1.03*	13.83±1.92*	6.57±0.34	9.53±0.56*
7	6.48±0.37	10.5±1.30*	9.22±0.73*	5.99±0.18	10.56±0.33*
8	7.02±0.53	9.79±1.75	15.53±1.06*	6.71±0.40	10.71±0.28*
9	6.63±0.39	8.99±1.25	14.94±0.75*	6.81±0.36	12.02±1.01*
10	6.77±0.49	10.94±1.82	8.33±0.63	6.99±0.31	14.77±0.33*
11	6.54±0.46	8.9±0.61*	14.72±1.17*	9.68±0.53*	5.56±0.27
12	6.63±0.48	10.78±0.51*	14.43±1.54*	10.98±0.27*	8.63±0.19*
13	6.56±0.44	10.56±1.77	14.62±2.58*	12.98±0.14*	5.93±0.29
14	6.52±0.41	10.36±1.00*	13.16±1.89*	23.46±0.34*	5.74±0.27
15	6.14±0.51	11±1.82*	14.02±2.49*	14.25±0.10*	5.31±0.44
16	6.36±0.40	10.3±1.26*	14.18±1.84*	13.06±0.30*	6.19±0.29
17	7.06±0.14	9.54±1.51	12.66±0.94*	6.81±0.53	5.73±0.44*
18	6.9±0.29	13.3±0.96*	11.94±1.37*	7.83±0.77	5.71±0.32*
19	6.61±0.47	8.98±0.24*	9.89±1.79	6.24±0.59	15.08±0.41*
20	7.1±0.46	10.84±1.54*	10.09±1.97	6.19±0.54	11.76±1.14*
21	6.64±0.41	9.2±1.72	13.42±1.68*	17.86±0.31*	5.92±0.47
22	6.88±0.27	9.82±1.30	10.04±1.60	16.81±2.14*	9.8±0.27*
23	6.96±0.30	9.46±1.25	12.14±2.40	6.29±0.19	14.45±0.14*
24	7.23±0.55	8.99±1.11	13.54±1.14*	15.7±0.40*	8.49±0.28
25	6.62±0.28	9.07±1.35	11.88±1.76*	17.72±0.59*	6.24±0.71
26	7.25±0.59	11.03±2.03	9.84±1.47	9.04±0.98	10.8±0.52*
27	6.87±0.73	13.31±1.07*	10.06±1.78	13.7±0.43*	15.76±1.19*
28	6.76±0.28	10.65±0.83*	11.1±1.36*	5.84±0.33	15.04±1.08*
29	7.02±0.56	11.02±1.32*	13.08±1.83*	6.49±0.27	5.46±0.67
30	6.67±0.56	9.28±1.67	11.68±1.73*	5.96±0.37	13.69±0.74*
31	6.92±0.41	10.21±1.75	12.45±1.64*	6.27±0.40	5.81±0.10*
32	14.56±1.26	7.43±0.41*	11.65±1.01	19.26±3.36	5.87±0.25*
33	6.76±0.50	11.65±1.44*	14.13±0.24*	6.09±0.40	5.87±0.33
34	5.74±0.38	7.54±0.97	15.46±0.33*	6.01±0.56	15.95±0.28*
35	6.83±0.49	10.21±1.32*	12.46±2.49	8.29±1.25	5.77±0.24
36	6.2±0.56	9.61±1.22*	10.18±1.59*	5.9±0.32	14.94±1.29*
37	6.64±0.98	9.04±1.10	10.37±0.25*	5.72±0.37	17.99±0.50*
38	6.82±0.70	10.44±1.91	10.11±0.77*	14.8±1.35*	5.04±0.57
39	6.77±0.48	11.63±1.99*	9.77±0.86*	13.77±2.57*	5.95±0.25
40	6±0.44	10.75±0.27*	11.32±1.29*	14.39±2.52*	5.59±0.42
41	6.64±0.55	9.1±1.05	10.74±0.46*	14.59±2.86*	5.7±0.39
42	6.86±1.00	9.52±1.05	9.34±0.05*	6.15±0.26	17.34±0.76*
43	8.08±0.42	10.58±1.50	11.53±0.79*	6.12±0.44*	13.29±0.42*
44	6.74±0.64	8.79±1.41	10.94±0.44*	5.77±0.19	14.08±0.51*

The results expressed as units of SOD activity calculated per milligram of protein. Values represent mean ± SEM of six independent experiments. Asterisks indicate significance of the differences against control ($P<0.05$).

Table A-4. Distribution of OGG1 activity across the mouse brain during exposure to MPTP (20 mg/kg, ip)

Punch Position	Control	12 hours	24 hours	48 hours	72 hours
1	9.91±2.77	19.6±1.37*	18.9±2.06*	16.5±2.99	17.8±5.30
2	6.15±1.06	19.3±5.32*	18.2±3.61*	19.8±2.93*	20.0±3.94*
3	7.45±1.63	12.8±3.31	15.6±3.59	16.0±2.10*	14.0±2.11*
4	6.35±0.86	18.0±2.00*	7.39±1.05	18.2±2.30*	36.4±1.78*
5	5.02±0.82	11.8±0.70*	13.6±1.42*	17.9±3.53*	18.6±1.26*
6	7.06±1.88	18.9±0.70*	12.0±2.00	19.3±2.32*	16.1±1.99*
7	7.55±1.11	17.7±1.79*	11.6±2.36	8.22±0.82	9.86±0.97
8	6.87±1.39	14.7±0.48*	14.4±3.88	13.2±2.08*	15.1±1.52*
9	5.87±0.91	14.5±2.53*	18.5±4.05*	15.3±2.72*	19.1±0.45*
10	5.87±1.68	16.0±0.94*	17.1±1.05*	8.38±0.76	11.1±2.63
11	4.61±0.97	14.9±2.37*	12.6±2.13*	9.52±1.00*	9.53±1.70*
12	7.41±1.23	14.4±2.54*	14.7±2.46*	11.7±1.37*	14.3±2.07*
13	5.88±1.38	15.1±1.67*	20.6±4.61*	16.4±1.73*	8.32±1.54
14	6.55±1.80	13.3±2.39	19.7±3.18*	27.0±1.75*	11.2±0.91
15	5.16±1.25	8.08±1.46	21.3±3.28*	26.8±3.27*	14.4±4.02
16	5.78±1.33	3.88±0.64	18.8±2.71*	27.3±1.87*	8.15±0.72
17	7.25±1.42	5.85±0.93	19.3±2.60*	15.0±0.39*	12.4±0.96*
18	5.77±1.77	7.24±0.89	18.8±3.22*	23.7±5.20*	8.68±0.54
19	7.89±0.97	10.1±0.08	19.1±2.60*	9.75±1.36	32.1±6.64*
20	7.97±1.14	10.0±0.38	12.0±1.16*	18.2±3.75*	16.2±1.41*
21	6.90±0.56	4.56±0.74*	14.9±1.90*	24.0±5.76*	7.75±0.81
22	7.50±1.13	6.56±1.51	10.0±2.73	9.31±1.33	17.4±2.54*
23	8.85±1.58	10.2±0.19	14.4±1.78*	13.5±2.73	14.5±2.27
24	11.7±1.15	9.29±1.56	11.7±2.46	25.8±2.34*	12.8±1.41
25	5.12±1.49	12.1±1.11*	15.6±2.38*	24.8±3.68*	14.8±0.27*
26	6.54±1.40	12.6±0.42*	19.3±3.06*	13.3±1.12*	24.3±2.54*
27	5.81±0.47	19.1±0.76*	12.3±0.65*	25.8±2.76*	16.3±2.24*
28	8.32±0.91	9.02±1.20	8.37±1.31	12.0±1.31*	9.45±0.91
29	7.77±1.59	17.5±0.38*	14.9±2.72	9.36±1.28	24.1±2.07*
30	4.57±1.21	11.8±2.17*	16.9±1.70*	7.98±0.64*	16.1±3.95*
31	10.6±0.52	5.22±1.19*	12.9±1.74	9.81±1.90	12.9±2.90
32	12.7±2.81	11.2±2.00	15.9±1.43	29.5±2.38*	11.4±0.31
33	7.69±0.94	7.29±1.44	12.9±2.18	13.9±0.46*	11.7±2.27
34	8.03±0.78	9.46±3.19	20.6±4.15*	10.9±1.65	20.3±3.94*
35	7.87±1.67	18.6±2.33*	15.0±1.17*	19.1±1.83*	10.4±1.17
36	7.61±1.67	12.3±0.37*	5.94±0.93	11.2±1.32	37.2±0.83*
37	5.38±0.61	12.0±0.69*	11.7±1.45*	20.2±2.06*	37.2±2.55*
38	7.09±1.22	18.5±2.27*	18.3±3.99*	25.2±1.64*	19.6±1.97*
39	7.29±1.66	7.42±2.01	9.20±1.08	17.3±1.01*	11.3±2.28
40	8.89±1.28	19.6±4.13*	12.0±1.35	17.1±0.43*	12.1±0.45
41	5.82±0.77	14.9±3.96	9.07±1.60	18.9±1.87*	13.4±1.35*
42	7.34±1.29	11.3±2.39	11.7±1.76	12.6±0.70*	15.7±3.08*
43	9.81±1.31	15.1±2.44	2.05±0.38*	12.4±0.68	17.8±3.35
44	9.00±1.96	17.1±2.73	15.9±1.95*	15.7±1.85*	21.7±3.34*

The results expressed as fmol of ^{32}P-labeled duplex oligonucleotide incised by per milligram of protein during 1 h. Values represent mean ± SEM of six independent experiments. Asterisks indicate significance of the differences against control ($P<0.05$).

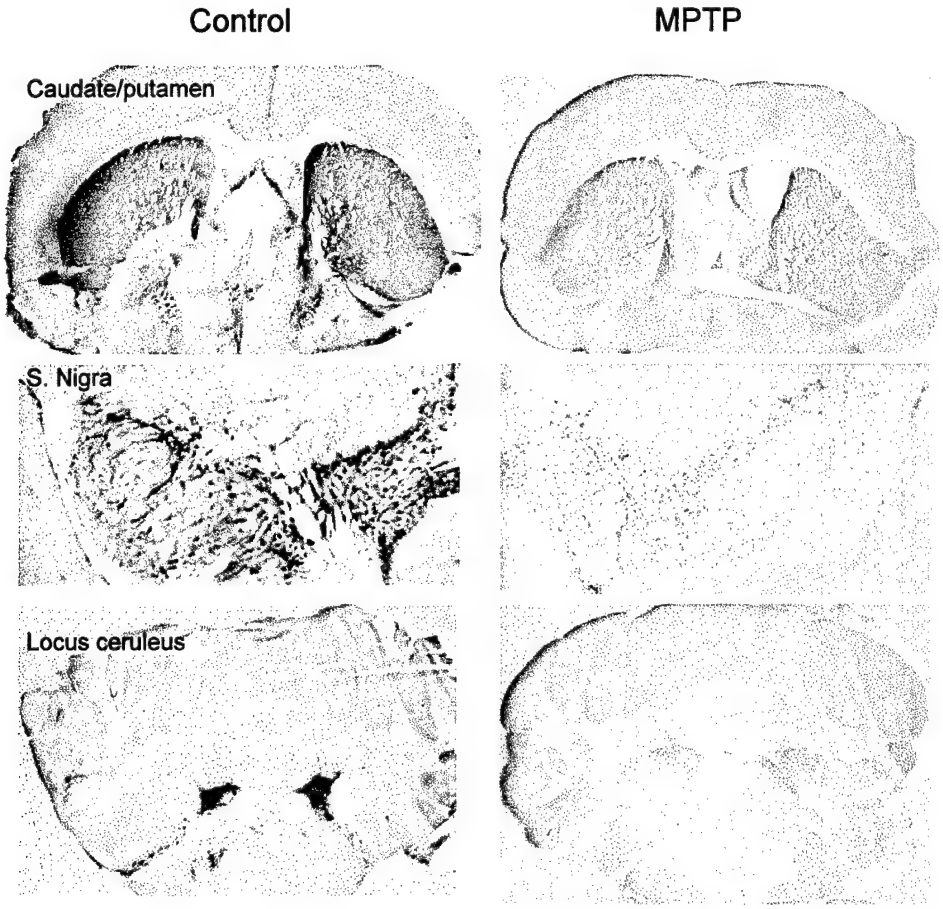

Figure A-1. Representative microphotographs of TH immunoreactivity in the Caudate/Putamen (striatum) in the upper panels, substantia nigra in the middle panels and locus ceruleus in the lower panels 72 hrs after MPTP (20 mg/kg, ip) treatment. Untreated controls are in the left-hand panels.

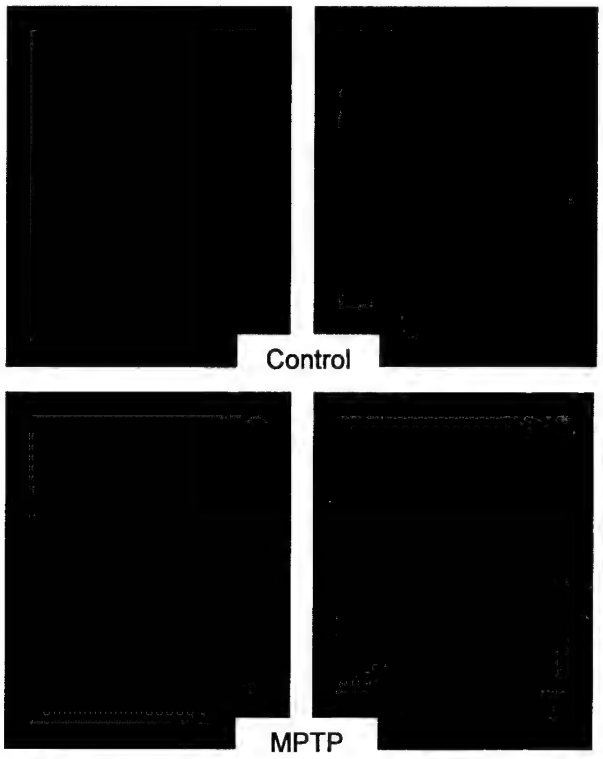

Figure A-2 Representative fluorescence microphotographs of TUNEL immunoreactivity in substantia nigra of mouse brain exposed to single dose of MPTP (20 mg.kg, ip). Left panels represent DAPI stained nuclei and right panels depict TUNEL-positive (apoptotic) cells. Upper panels represent control and lower ones were obtained from animals after 72 h of intoxication. The positively labeled cells were identified with Olympus fluorescence microscope (magnification was x 200).

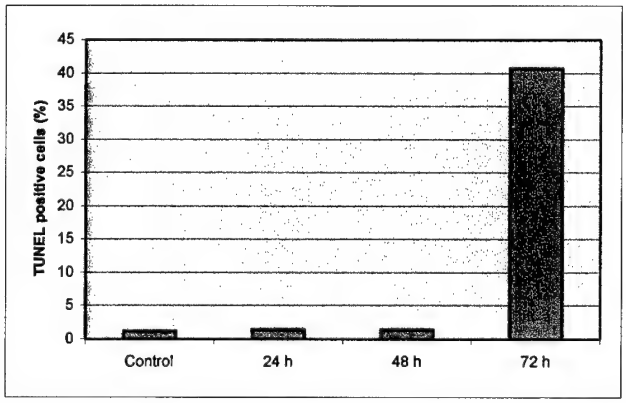

	Control	24 h	48 h	72 h
Mean	1.185	1.45	1.458	40.663
SEM	0.6296	0.2118	0.2044	2.2766

Figure A-3 Number of TUNEL-positive cells in the substantia nigra in time course of intoxication caused by ip injection of single dose of MPTP (20 mg/kg). The numbers of cells per animal were averaged in 3 sections performed for 3 animals of each group (Control, 24, 48 and 72 hours). Data expressed as mean ± SEM. The extent of TUNEL-positive immunostaining was calculated as ratio between green fluorescent cells and DAPI blue stained nucleus. Statistical significance was assumed at $P<0.05$.

Gene Expression, Vol. 11, pp. 211-219

Rubratoxin B Elicits Antioxidative and DNA Repair Responses in Mouse Brain

V. Sava,[1,2] *D. Mosquera,*[1,2] *S. Song,*[1,2] *T. Stedeford,*[2,4] *K. Calero,*[1] *F. Cardozo-Pelaez,*[3] *R. Harbison,*[4] *and J. Sanchez-Ramos*[1,2]

[1]Neurology, University of South Florida, Tampa, FL
[2]Research Service, James Haley VA, Tampa, FL
[3]Department of Pharmaceutical Sciences, University of Montana, Missoula, MT
[4]College of Public Health, University of South Florida, Tampa, FL

Rubratoxin B (RB) is a mycotoxin with potential neurotoxic effects that have not yet been characterized. Based on existing evidence that RB interferes with mitochondrial electron transport to produce oxidative stress in peripheral tissues, we hypothesized that RB would produce oxidative damage to macromolecules in specific brain regions. Parameters of oxidative DNA damage and repair, lipid peroxidation, and superoxide dismutase (SOD) activity were measured across six mouse brain regions 24 h after administration of a single dose of RB. Lipid peroxidation and oxidative DNA damage were either unchanged or decreased in all brain regions in RB-treated mice compared with vehicle-treated mice. Concomitant with these decreased indices of oxidative macromolecular damage, SOD activity was significantly increased in all brain regions. Oxyguanosine glycosylase activity (OGG1), a key enzyme in the repair of oxidized DNA, was significantly increased in three brain regions--cerebellum (CB), caudate/putamen (CP), and cortex (CX)--but not in the hippocampus (HP), midbrain (MB), and pons/medulla (PM). The RB-enhanced OGG1 catalytic activity in these brain regions was not due to increased OGG1 protein expression, but was a result of enhanced catalytic activity of the enzyme. In conclusion, specific brain regions responded to an acute dose of RB by significantly altering SOD and OGG1 activities to maintain the degree of oxidative DNA damage equal to, or less than, that of normal steady-state levels.

Key words: Rubratoxin B; Oxidative stress; DNA damage and repair; Superoxide dismutase (SOD); Mouse brain regions

Address correspondence to Dr. Juan R. Sanchez-Ramos, The Helen E. Ellis Professor of Neurology, University of South Florida, Department of Neurology (MDC 55), 12901 Bruce B. Downs Blvd., Tampa, FL 33612. Tel: (813) 974-6022; Fax: (813) 974-7200; E-mail: jsramos@hsc.usf.edu

DISTRIBUTION OF OXIDATIVE DNA DAMAGE AND OXYGUANOSINE GLYCOSYLASE ACTIVITIES ACROSS BRAIN REGIONS OF MICE INJECTED WITH A SINGLE DOSE OF RUBRATOXIN - B. *Society for Neurosciences Ab 669.4, 2003*

V.Sava[1,2]; *D.Mosquera[1,2]; S.Song[1,2]; K.Calero[1]; R.Harbison[4]; F.Cardozo-Pelaez[3]; J.Sanchez-Ramos[1,2*]*

1. Neurol., Univ. of South Florida, Tampa, FL, USA

2. Res. Service, James Haley VA, Tampa, FL, USA

3. 2Department of Pharmaceut. Sci., Univ. of Montana, Missoula, MT, USA

4. Col. of Public Hlth., Univ. of South Florida, Tampa, FL, USA

Rubratoxin B (RB) is a potent neurotoxicant with an undefined mechanism of toxicity. Hypothesizing that oxidative DNA damage might underlie neurotoxicity, steady-state levels of 8-oxoguanine (8-oxodG) and oxyguanosine glycosylase (OGG1) activity were measured in cerebellum (CB), cortex (CX), hippocampus (HP), midbrain (MB), caudate/putamen (CP) and pons/medulla (PM) of Swiss ICR mice. Oxidative DNA damage (measured by 8-oxodG levels)was paradoxically decreased relative to control samples across all brain regions 24 h after administration of RB (5 mg/kg). OGG1 activities, indicative of DNA repair, were increased in CB, CP and CX in RB-treated mice compared to non-treated controls. The OGG1 activity in specific brain regions was inversely proportional to regional DNA damage with a correlation factor of 0.9545. The decrease in 8-oxodG was also associated with increased superoxide dismutase (SOD) activity. Native PAGE of the protein extracts from brain regions demonstrated two distinct bands with the enzymatic capacity to cleave 32P-labeled duplex oligonucleotide containing 8-oxodG. These bands were attributed to different isoforms of OGG1. Computer modeling was applied to generate kinetic curves representing the experimental data as a superimposition of two enzymatic isoforms of OGG1. To summarize, specific brain regions responded to an acute dose of RB by significantly increasing DNA repair activity and decreasing the steady-state levels of 8-oxodG. Ongoing work is examining the regulation of OGG1 mRNA expression in specific neuronal populations at 6 and 12 hrs after exposure to RB.

Support Contributed By: Dept of Defense Grant #DAMD17-03-1-0501 and *VA Merit Review Grant*

DOPAMINERGIC NEUROTOXICITY ASSOCIATED WITH DEFICIT IN REPAIR OF OXIDATIVE DNA DAMAGE CAUSED BY OCHRATOXIN-A *Society for Neurosciences Ab in press 2004*

V. Sava[1,2]; A. Velasquez[1,2]; S. Song[1,2]; J. Sanchez-Ramos[1,2]*

1. Neurology, University of South Florida, Tampa, FL, USA 2. Research Service, James Haley VA, Tampa, FL, USA

Ochratoxin A (OTA) is a mycotoxin with poorly understood neurotoxicant effects. Hypothesizing that the neurotoxicity of OTA is associated with deficient repair of oxidative DNA damage in specific neuronal populations, we measured the acute effects of OTA on the activity of the DNA repair enzyme, oxyguanosine glycosylase (OGG1), in cerebellum (CB), cortex (CX), hippocampus (HP), midbrain (MB), caudate/putamen (CP) and pons/medulla (PM) of Swiss ICR mice. DA and its metabolites, homovanillic acid and (HVA) dihydroxyphenylacetic (DOPAC) were also measured by HPLC in the same regions. Mice received 5 doses i.p. of OTA (0.37 to 6 mg/kg) resulting in a dose-dependent depletion of DA with the greatest effect in CP and frontal cortex. The highest dose (6 mg/kg) caused a 6 fold decrease of DA concentration in CP. The ED50 for DA depletion ranged between 3 and 4 mg/kg. OGG1 activities, indicative of DNA repair, were changed in specific brain regions in OTA-treated mice compared to non-treated controls. Levels of OGG1 activity were associated with changes in DA, HVA and DOPAC concentration. Modulation of OGG1 activity by OTA and its effects on DA content may provide new insights into the pathogenesis of Parkinson's disease.

Supported by: Dept of Defense Grant #DAMD17-03-1-0501 and VA Merit Review Grant

Gene Expression, Vol. 11, pp. 211–219
Printed in the USA.

1052-2166/04 $20.00 + .00

Rubratoxin B Elicits Antioxidative and DNA Repair Responses in Mouse Brain

V. SAVA,*† D. MOSQUERA,*† S. SONG,*† T. STEDEFORD,†§ K. CALERO,* F. CARDOZO-PELAEZ,‡ R. HARBISON,§ AND J. SANCHEZ-RAMOS*†[1]

*Neurology, University of South Florida, Tampa, FL
†Research Service, James Haley VA, Tampa, FL
‡Department of Pharmaceutical Sciences, University of Montana, Missoula, MT
§College of Public Health, University of South Florida, Tampa, FL

Rubratoxin B (RB) is a mycotoxin with potential neurotoxic effects that have not yet been characterized. Based on existing evidence that RB interferes with mitochondrial electron transport to produce oxidative stress in peripheral tissues, we hypothesized that RB would produce oxidative damage to macromolecules in specific brain regions. Parameters of oxidative DNA damage and repair, lipid peroxidation, and superoxide dismutase (SOD) activity were measured across six mouse brain regions 24 h after administration of a single dose of RB. Lipid peroxidation and oxidative DNA damage were either unchanged or decreased in all brain regions in RB-treated mice compared with vehicle-treated mice. Concomitant with these decreased indices of oxidative macromolecular damage, SOD activity was significantly increased in all brain regions. Oxyguanosine glycosylase activity (OGG1), a key enzyme in the repair of oxidized DNA, was significantly increased in three brain regions—cerebellum (CB), caudate/putamen (CP), and cortex (CX)—but not in the hippocampus (HP), midbrain (MB), and pons/medulla (PM). The RB-enhanced OGG1 catalytic activity in these brain regions was not due to increased OGG1 protein expression, but was a result of enhanced catalytic activity of the enzyme. In conclusion, specific brain regions responded to an acute dose of RB by significantly altering SOD and OGG1 activities to maintain the degree of oxidative DNA damage equal to, or less than, that of normal steady-state levels.

Key words: Rubratoxin B; Oxidative stress; DNA damage and repair; Superoxide dismutase (SOD); Mouse brain regions

MYCOTOXINS are toxic fungal metabolites that are structurally diverse, common contaminants of the ingredients of animal feed and human food. These fungal products exhibit a range of pharmacological activities that have been utilized in development of mycotoxins or mycotoxin derivatives as antibiotics, growth promoters, and other kinds of drugs; still others have been developed as biological and chemical warfare agents (1). Bombs and ballistic missiles laden with biological agents, including mycotoxins, are believed to have been deployed by Iraq during Operation Desert Storm (23). In light of the excess incidence of amyotrophic lateral sclerosis in young Gulf War veterans (7), it is important not to forget the potential neurotoxic effects of low doses of mycotoxins. Although much is known about the lethal effects of the aflatoxins, little is known about the acute and long-term effects of rubratoxin B (RB) on the adult nervous system.

RB is a metabolite of the molds *Penicillum rubrum* and *Penicillum purpurogenum*. These molds commonly contaminate cereals and foodstuffs and grow on damp tents and fabrics. RB is not known to produce a serious health hazard in this naturally occurring form, but pure RB is a bisanhydride lactone with hepatotoxic (17) and teratogenic properties (10–12). Investigation of the effects of acute and chronic exposure to RB on the nervous system has been scarce,

[1]Address correspondence to Dr. Juan R. Sanchez-Ramos, The Helen E. Ellis Professor of Neurology, University of South Florida, Department of Neurology (MDC 55), 12901 Bruce B. Downs Blvd., Tampa, FL 33612. Tel: (813) 974-6022; Fax: (813) 974-7200; E-mail: jsramos@hsc.usf.edu

even though neuronal tissue appears to be very susceptible to the deleterious effect of RB in teratogenic studies (9).

RB has numerous biochemical actions including the inhibition of (Na^+-K^+)-ATPase (18), inhibition of the hepatic cytochrome P-450-dependent monooxygenase system (19), reduction of hepatic and renal nonprotein sulfhydryl content (6), and inhibition of gap junctional intercellular communication (16). It was found that RB caused shifts in the ultraviolet absorption spectra of DNA and RNA (21). The observed binding properties of RB can disrupt the integrity of DNA and RNA. RB has been shown to induce apoptosis (14,15) and internucleosomal fragmentation of DNA (14).

Studies with isolated mouse liver mitochondria revealed that RB disrupted mitochondrial respiration and depressed oxygen consumption (9). The principal site of action of RB in the mitochondrial electron transport system was found to be between cytochrome C1 and the termination of electron flow (9). Ochratoxin, a related mycotoxin, has been reported to alter mitochondrial respiration and oxidative phosphorylation through impairment of the mitochondrial membrane and inhibition of the succinate-dependent electron transfer activities of the respiratory chain (22).

The overall objective was to study RB neurotoxicity in the context of oxidative stress induced by inhibition of mitochondrial electron transport in brain tissues. Inhibition of oxidative phosphorylation would be expected to result in increased generation of oxyradicals and decreased production of ATP (8). We hypothesized that RB-induced alteration of oxidative processes would not be homogeneous across all brain regions but would reflect the capacity of distinct brain regions to upregulate antioxidative mechanisms and repair processes. Parameters of oxidative stress measured included lipid peroxidation (thiobarbituric acid-reactive substances or TBARS), superoxide dismutase (SOD) activity, oxidative DNA damage and repair in each of six brain regions: cerebellum (CB), cortex (CX), hippocampus (HP), midbrain (MB), caudate/putamen (CP), and pons/medulla (PM). Accumulation of 8-oxodG was chosen as an indicator of DNA damage, and activity of DNA glycosylase was used as an index of DNA repair.

MATERIALS AND METHODS

Materials

RB, SOD, xantine oxidase, ribonuclease T1, HEPES, dithiotreitol (DTT), bovine serum albumin, and acrylamide/bisacrylamide (19:1) mixture were purchased from Sigma (St. Louis, MO). TEMED was from Bio-Rad Laboratories (Hercules, CA). Protease inhibitors and 8-oxoguanine DNA glycosylase (mOGG1) were from Boehringer Mannheim (Indianapolis, IN). Synthetic oligonucleotide containing 8-oxodG was from Trevigen (Gaithersburg, MD). [^{32}P]ATP (7000 Ci/mmol) was from ICN Biomedical, Inc. (Costa Mesa, CA). Phosphorylation buffer, 3′-phosphate-free T4 polynucleotide kinase, RNase, proteinase K, nuclease P1, and alkaline phosphatase were from Roche Diagnostic Co. (Indianapolis, IN). G-25 Microcentrifuge Spin Column was from Shelton Scientific (Shelton, CT). mOGG1 antibody was from Alpha Diagnostic (San Antonio, TX). ECL Western blotting analysis system was from Amersham Biosciences (Piscataway, NJ). All other reagents were ACS grade and from Sigma Chemical Co.

Animals and Treatment

The animal protocol used in this study was approved by the University of South Florida (USF) IUCAC committee. The protocol was also reviewed and approved by the USF Division of Comparative Medicine, which is fully accredited by AAALAC International and managed in accordance with the Animal Welfare Regulations, the PHS Policy, the FDA Good Laboratory Practices, and the IACUC's Policies. Male Swiss ICR mice (22 ± 2 g) were obtained from Jackson Laboratories (Bar Harbor, ME). They were housed five per cage at the temperature of 21 ± 2°C with 12-h light/dark cycle and free access to food and water. Mice were divided into experimental (n = 10) and control (n = 5) groups. Animals were injected with either RB dissolved in DMSO (5 mg/kg, IP) or vehicle. Mice were sacrificed with CO_2 24 h after treatment. The brains were removed and immediately dissected in a petri dish on ice (4°C).

Isolation of Brain Regions

The brain was separated into six regions under a dissecting microscope in the following order. The cerebellar peduncles were cut first, and the brain stem was removed from the diencephalon. The ventral and dorsal parts of the midbrain (MB) were dissected at the level of the caudal end of the cerebral peduncles at the junction with the pons. The pons and medulla (PM) were separated together by cutting the ponto–medullary junction. The cerebral hemispheres were opened with a sagittal cut along the longitudinal tissue and the hippocampus (HP) was isolated, followed by caudate and putamen (CP). Finally, the cerebellum (CB) and cerebral cortex (CX) were harvested and all the samples were kept frozen at −70°C until assay.

Measurement of DNA Damage

Steady-state level of 8-oxodG was used as a marker of oxidative DNA damage. The procedure for DNA isolation was basically the same as reported previously (2). Approximately 150 mg of brain sample was used for extraction. Briefly, tissue was pulverized in liquid nitrogen, using mortar and pestle, sonicated in 10 mM ethylenediamine tetraacetic acid (EDTA), and centrifuged. The pellet was treated with DNAase-free RNAase followed by digestion with proteinase K. The protein fraction was separated from DNA by three consecutive organic extractions. The DNA was precipitated by ethanol and incubated overnight at −20°C. The ratio in absorbance at 260/280 nm was employed for qualification of DNA purity.

The purified DNA was digested with nuclease P1 followed by treatment with alkaline phosphatase. The mixture of deoxynucleosides was analyzed with HPLC using 5% methanol dissolved in 100 mM of sodium acetate (pH 5.2) as a mobile phase, and 8-oxodG was detected with an electrochemical detector (ESA Coulochem Model 5100A) at +0.4 V. 2-dG was detected at 260 nm in the same sample using a Perkin Elmer 785A Programmable Absorbance Detector (Perkin Elmer, Norwalk, CT) connected in series with the electrochemical detector. 8-oxodG level was expressed as ratio of 8-oxodG/2-dG. Data were recorded, stored, and analyzed on a PC Pentium computer using ESA 500 Chromatography Data System Software.

Assessment of OGG1 Activity

The extraction of OGG1 for enzymatic assay was performed as described previously (2). Briefly, brain tissue was pulverized in liquid nitrogen, using mortar and pestle. Homogenization buffer contained 20 mM Tris-base (pH 8.0), 1 mM EDTA, 1 mM DTT, 0.5 mM spermine, 0.5 mM spermidine, 50% glycerol, and protease inhibitors. Homogenates were rocked for 30 min after addition of 1/10 volume 2.5 M KCl and spun at 14,000 rpm for 30 min. The supernatant was aliquoted and specimens were kept frozen at −70°C until assay. Protein concentration was measured using the bicinchoninic acid (20).

OGG1 activity was measured by incision assay as previously described (2). To prepare ^{32}P-labeled duplex oligonucleotide, 20 pmol of synthetic probe containing 8-oxodG (Trevigen, Gaithersburg, MD) was incubated at 37°C with [^{32}P]ATP and polynucleotide T4 kinase. To separate the unincorporated free [^{32}P]ATP, the reaction mixtures were spun through a G25 spin column. Complementary oligonucleotides were annealed in 10 mM Tris (pH 7.8), 100 mM KCl, 1 mM EDTA by heating the samples 5 min at 80°C and gradually cooling at room temperature.

Incision reaction (20 µl) contained 40 mM HEPES (pH 7.6), 5 mM EDTA, 1 mM DTT, 75 mM KCl, purified bovine serum albumin, 100 fmol of ^{32}P-labeled duplex oligonucleotide, and protein extract (30 µg). The reaction mixture was incubated at 37°C for 2 h and placed on ice to terminate the reaction. Then 20 µl of loading buffer containing 90% formamide, 10 mM NaOH, and blue-orange dye was added to each sample. After 5 min of heating at 95°C the samples were resolved in a denaturing 20% polyacrylamide gel containing 7 M urea. The gel was visualized using Biorad-363 Phosphoimager System, and OGG1 incision activity was calculated as the amount of radioactivity in the band corresponding to the specific cleavage product over the total radioactivity in the lane.

Kinetic Study of OGG1 Incision Reaction

Reaction mixtures and conditions used for kinetic studies were identical to OGG1 incision activity assay, but amounts of the appropriate ^{32}P-labeled oligonucleotide duplex were varied. The enzyme concentration and reaction time was adjusted to cleave no more than 10% of the substrate. Kinetic parameters were calculated using a Jandel SigmaPlot version 5.00 nonlinear fit routine. Three independent experiments were performed for each analysis.

Western Immunoblotting

The 8-oxoguanine DNA glycosylases extracted from different regions of brain were separated on a 12% SDS-PAGE and transferred onto a nitrocellulose membrane using a Biorad Semi-Dry Transblot technique. The membranes were blocked overnight at 4°C in a solution containing 5% dry milk and Tris-buffered saline (TBS) composed of 200 mM NaCl and 50 mM Tris-HCl (pH 7.4), and supplemented with 0.04% Tween-20. The membranes were rinsed in TBS-Tween mixture and incubated overnight at 4°C with mOGG1 antibody (Alpha Diagnostic, TX) using 1:1000 dilution by 1% dry milk prepared on TBS-Tween. After washing (3 × 10 min) with TBS-Tween at 4°C, the membranes were incubated with goat anti-mouse antibody (1:2000 dilution) conjugated to horseradish peroxidase (Santa Cruz Biotechnology, CA) for 1 h at room temperature. The blot was developed by ECL kit (Amersham Biosciences, Piscataway, NJ).

Native PAGE

OGG1 extracted from different regions of the brain was mixed with native buffer composed of 0.1 M Tris-HCl (pH 6.8), 30% glycerol, and 0.01% bromo-

phenol blue and separated on a nondenaturing 10% polyacrylamide gel at 120 V. Gel was sliced by a razor blade along the lanes into sections 1 mm thick. A single 1-mm-thick section was homogenized with a Teflon hand homogenizer in 20 µl of incision reaction mixture and enzymatic activity of OGG1 was assayed as described above.

Lipid Peroxidation

Formation of lipid peroxide derivatives was evaluated by measuring thiobarbituric acid-reactive substances (TBARS) according to Cascio et al. (3). Briefly, the different regions of the brain were individually homogenized in ice-cold 1.15% KCl (w/v). Then 0.4 ml of the homogenates was mixed with 1 ml of 0.375% TBA, 15% TCA (w/v), 0.25 N HCl, and 6.8 mM butylated-hydroxytoluene (BHT), placed in a boiling water bath for 10 min, removed, and allowed to cool on ice. Following centrifugation at 3000 rpm for 10 min, the absorbance in the supernatants was measured at 532 nm. The amount of TBARS produced was expressed as nanomole TBARS per milligram of protein using malondialdehyde bis-(dimethyl acetal) for calibration.

SOD Assay

Determination of SOD activity in mouse brain regions was based on inhibition of nitrite formation in reaction of oxidation of hydroxylammonium with superoxide anion radical (5). Nitrite formation was generated in a mixture containing 25 µl xanthine (15 mM), 25 µl hydroxylammonium chloride (10 mM), 250 µl phosphate buffer (65 mM, pH 7.8), 90 µl distilled water, and 100 µl xanthine oxidase (0.1 U/ml) used as a starter of the reaction. Inhibitory effect of inherent SOD was assayed at 25°C during 20 min of incubation with 10 µl of brain tissue extracts. Determination of the resulting nitrite was performed upon the reaction (20 min at room temperature) with 0.5 ml sulfanilic acid (3.3 mg/ml) and 0.5 ml α-naphthylamine (1 mg/ml). Optical absorbance at 530 nm was measured with Ultrospec III spectrophotometer (Pharmacia, LKB). The results were expressed as units of SOD activity calculated per milligram of protein. The amount of protein in the samples was determined using bicinchoninic acid (20).

Statistical Analysis

The results were reported as mean ± SE for at least five different preparations, assayed in duplicate. For electrophoresis two different gels were run. The differences between samples were analyzed by the Student's t-test, and a $p < 0.05$ was considered as statistically significant.

RESULTS

Administration of RB to mice (5 mg/kg body weight, IP) was chosen on the basis of a dose–toxicity curve (data not shown). That dose produced significant immobilization and decrease body temperature of animals. However, it resulted in no visible gross damage to brain but altered brain biochemistry. Namely, lipid peroxidation, indicated by TBARS levels, was decreased in all regions of the brain of the animals exposed to RB compared with control mice (Fig. 1). In HP, MB, and PM the TBARS levels were significantly ($p < 0.05$) different from the control. In the PM region, a 2.2-fold decrease in TBARS was observed.

Oxidative DNA damage, indicated by steady-state levels of 8-oxodG, showed a trend towards decreased

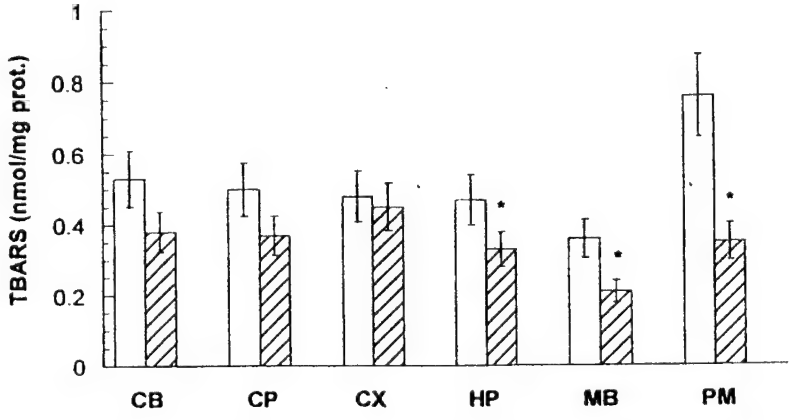

Figure 1. Content of TBARS in different regions of mouse brain exposed to RB (striped bars) in comparison with control (opened bars). All values represent mean ± SE. The significantly ($p < 0.05$) different levels of TBARS in comparison with control are indicated by asterisks.

TABLE 1
EVALUATION OF OXIDATIVE DNA DAMAGE, OXIDATIVE DNA REPAIR (OGG1), AND SUPEROXIDE DISMUTASE ACTIVITIES ACROSS DIFFERENT REGIONS OF MOUSE BRAIN EXPOSED TO RB IN COMPARISON WITH CONTROL

Brain Region	Animal Group	DNA Damage (ppm)	OGG1 Incision Activity (pM min^{-1} mg $prot^{-1}$)	Activity of SOD (U/mg prot.)
CB	control	18.4 ± 2.2	2.6 ± 0.2	42.5 ± 4.6
	RB intoxication	16.7 ± 2.1	4.06 ± 0.55*	63.8 ± 7.5*
CP	control	20.6 ± 3.8	3.05 ± 0.24	42.4 ± 2.7
	RB intoxication	18.2 ± 1.8	4.27 ± 0.45*	72.6 ± 6.1*
CX	control	20.7 ± 0.8	2.52 ± 0.4	34.8 ± 1.5
	RB intoxication	20.1 ± 5.1	3.86 ± 0.32*	64.5 ± 11.25*
HP	control	19.4 ± 1.2	2.86 ± 0.31	32.6 ± 3.2
	RB intoxication	16.1 ± 1.9	3.42 ± 0.33	78.14 ± 12.1*
MB	control	26.9 ± 8.3	2.79 ± 0.22	48.6 ± 2.1
	RB intoxication	20.2 ± 6.4	2.43 ± 0.19	112.5 ± 16.4*
PM	control	33.0 ± 2.4	3.4 ± 0.26	38.7 ± 3.8
	RB intoxication	22.7 ± 0.9*	3.0 ± 0.27	105.5 ± 14.8*

Values represent mean ± . The extent of DNA damage was calculated from the amount of 8-oxodG (fmol) contained in 1 nmol of 2-dG and expressed as parts per million (ppm).
*Significantly ($p < 0.05$) different compared with controls.

levels across all brain regions (Table 1). Statistically significant differences in 8-oxod-dG were found only in the PM region, where levels were reduced to 30% below control. Oxidative damage in the MB was also distinctly decreased, but did not reach statistical significance.

The decreased levels of oxidative DNA damage were associated with increased activity of the repair enzyme OGG1 (Table 1). There was a statistically significant increase in OGG1 activity in the CB, CP, and CX regions compared with the respective controls. In the HP the activity of OGG1 was higher than in control, though the difference did not reach statistical significance. Overall, the relative extent of DNA damage decreased linearly (Fig. 2) with relative activity of OGG1 (correlation factor was –0.9545). For both specific OGG1 and 8-oxodG relative indices were calculated as: relative indices = $100 \times (V_{RB} - V_C)/V_C$, where V_{RB} are values obtained in RB experiment and V_C in control.

The results in Table 1 demonstrated upregulation of SOD activity in RB-treated animals compared with control. The extent of increased SOD activity in different regions of the brain revealed a negative correlation with the level of 8-oxodG. Namely, the association between 8-oxodG and SOD activity can be expressed by the linear equation with the correlation factor of –0.8521: 8-oxodG = $-0.19 \times (SOD) + 4.6$.

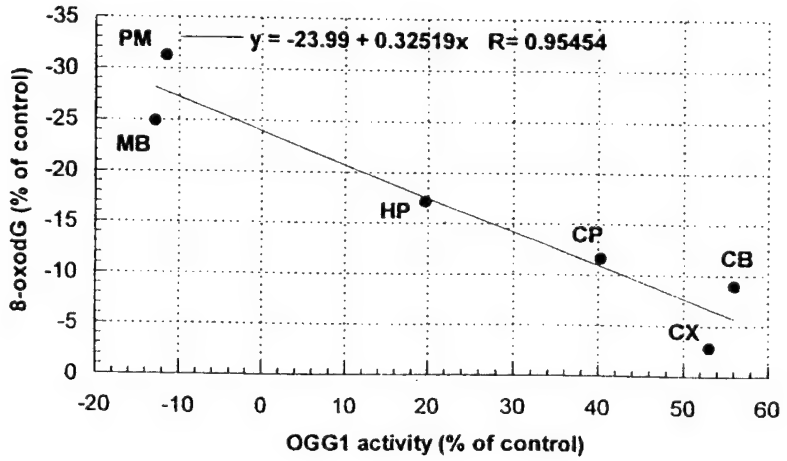

Figure 2. Relationship between relative indices of OGG1 activity and accumulation of 8-oxodG in various regions of mouse brain. Relative indices represent values normalized to the correspondent controls.

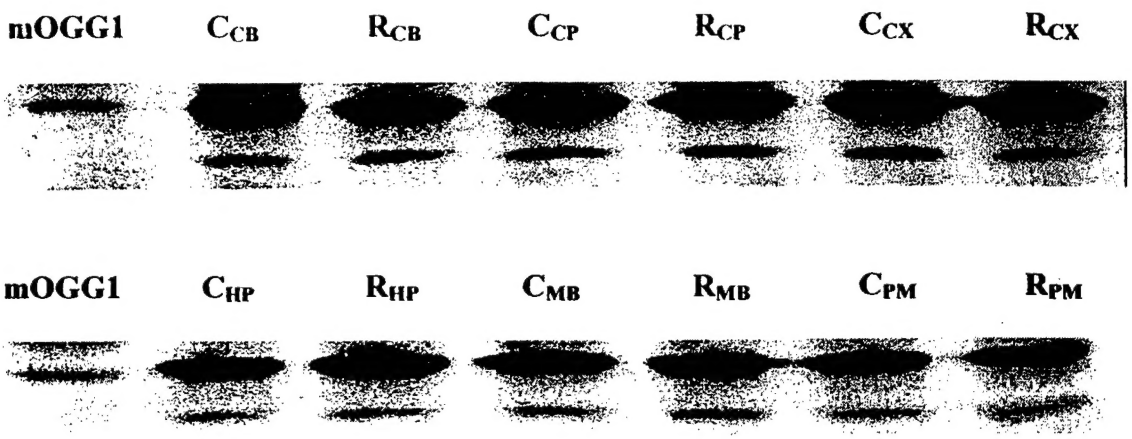

Figure 3. OGG1 expression in different regions of mouse brain. The Western blot lanes depicted by C_{CB}–C_{PM} array show the level of OGG1 in control mouse, and lanes from R_{CB} to R_{PM} represent OGG1 expression in the brain of RB-intoxicated animal. Pure enzyme presented as a positional marker for OGG1 identification.

Western blot analysis was carried out to elucidate the source of OGG1 activity (Fig. 3). It was found that protein expression levels of OGG1 were not significantly affected by RB exposure and there were no differences in regional levels of OGG1 when normalized to the total protein variations. One of the bands in the Western blot attributed to OGG1 matched the single band of pure enzyme. However, we found an additional band that was also labeled with OGG1 antibody. This band may be due to nonspecific binding with antibody or otherwise caused by existence of various isoforms of OGG1. To clarify this issue, we resolved OGG1 in native PAGE followed by cutting the gel into 1-mm strips and assaying the strips for OGG1 enzymatic (incision) activity. Figure 4 indicates the presence of two distinct bands with incision activity, which likely can be attributed to different isoforms of OGG1. Assaying the pure enzyme with

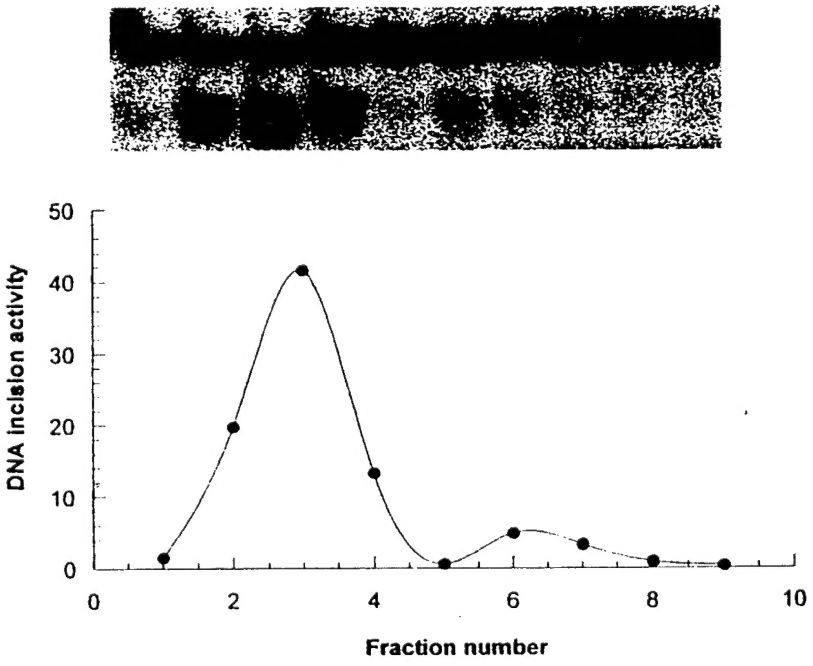

Figure 4. Determination of OGG1 on native PAGE. Enzymatic activity of OGG1 was assayed in every single fraction by using ^{32}P-duplex oligonucleotide. Upper panel represents ^{32}P-duplex oligonucleotide products visualized with Biorad-363 Phosphoimager System. Lower panel represent the averaged data of three experiments with OGG1 extracted from HP of control mouse. OGG1 activity was calculated as the percent of radioactivity in the band of specifically cleaved product over the total radioactivity in the lane.

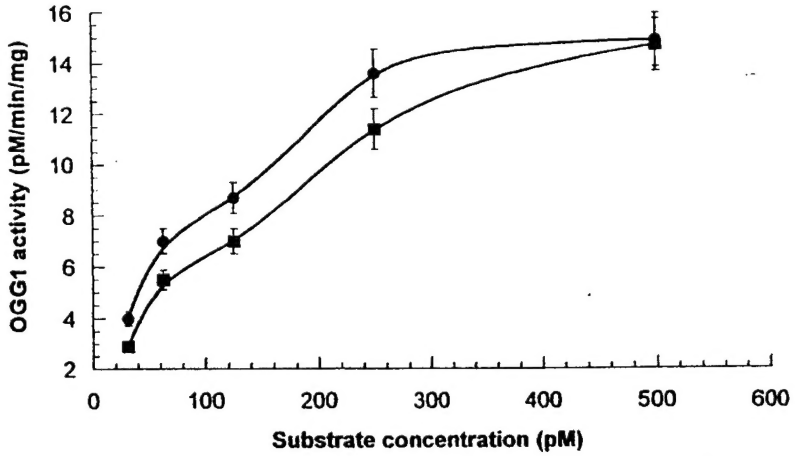

Figure 5. Kinetic behavior of OGG1 extracted from different regions of brain. Circles represent OGG1 obtained from CP of mouse exposed to RB. Squares represent OGG1 obtained from CP of control mouse. Data expressed by means of three replications.

the same procedure showed one single band possessing electrophoretic mobility identical to the major band of the tested sample (not shown).

The data are in agreement with kinetic behavior of OGG1 extracted from mouse brain. As can be seen from Figure 5, the oligonucleotide incision activity plotted against concentration reveals bimodal curves. The first part of incision activity reached saturation level in a range between 0 and 120 pM of substrate, but the second part needed higher concentrations of substrate (up to 500 pM). Computer modeling generated kinetic curves representing the experimental curve as a superposition of low- and high-saturated enzymatic isoforms. Separated incision activities were analyzed using Michaelis-Menten kinetics with the corresponding calculation of kinetic constants as shown in Table. 2.

DISCUSSION

Until the present report, the toxic effects of RB in adult brain had not been investigated. Administration of a single dose (5 mg/kg, IP) did not produce gross pathological changes in the brain, but resulted in paradoxically less oxidative damage to both lipids and DNA. In fact, the level of lipid peroxidation in the HP, MB, and PM was significantly less than that found in vehicle-treated controls. Similarly, RB did not increase oxidative DNA damage in any region of the brain after the injection but rather tended to lower the degree of damage. These results were unexpected in light of the putative pro-oxidant effects of the mycotoxin, but were explained by the robust upregulation of antioxidative and repair systems. RB treatment elicited an increase in activity of SOD, a major oxyradical scavenger, across all brain regions. In addition, measures of oxidative DNA repair were observed to increase in three of six brain regions following RB treatment.

Measurement of oxidative DNA damage revealed a trend towards decreased steady-state levels of 8-oxodG across all brain regions with a statistically significant decreased level in the PM. The DNA repair response assessed from the change in OGG1 activity was significantly increased in three brain regions (CX, CB, CP) but it is noteworthy that maintenance of normal steady-state levels of 8-oxodG was facili-

TABLE 2
KINETIC CHARACTERIZATION OF OGG1 ISOFORMS OBTAINED FROM CP OF CONTROL MOUSE AND FROM CP OF MOUSE SUBJECTED TO RB

		Kinetic Constants		
Isoform of OGG1	Samples Tested	K_m (pM)	V_{max} (pM min^{-1} mg^{-1})	V_{max}/K_m (min^{-1} mg^{-1})
High saturated	CP exposed to RB	147.7 ± 12	20.1 ± 2.1	0.136 ± 0.01
	CP control	312.9 ± 29	24.7 ± 2.6	0.078 ± 0.007
Low saturated	CP exposed to RB	105.3 ± 9	17.7 ± 2	0.16 ± 0.02
	CP control	140.5 ± 11	16.2 ± 1.5	0.11 ± 0.01

tated by the greatly enhanced SOD activity in regions of the brain where OGG1 did not increase.

The index of DNA damage utilized in this study was 8-oxodG, a major premutagenic DNA lesion generated from the reaction of oxyradicals with guanosine. Repair of this DNA lesion involves DNA *N*-glycosylases that hydrolyze the *N*-glycosylic bond between the 8-oxoG and deoxyribose, releasing the free base and leaving an apurinic/apyrimidinic (AP) site in DNA. Such AP sites are cytotoxic and mutagenic, and must be further processed. Some DNA glycosylases also have an associated AP lyase activity that cleaves the phosphodiester bond 3′ to the AP site (13). Formamidopyrimidine glycosylase (fpg, also named fapy-DNA glycosylase) is a prokaryotic protein originally identified in *E. coli* that catalyzes the excision of damaged purine bases such as 8-oxodG and 2,6-diamino-4-hydroxy-5-*N*-methylformamidopyrimidine from double-stranded DNA. Two distinct homologues of fpg were identified in yeast, OGG1 and OGG2 (8-oxo-guanine glycosylase). The counterpart of yeast OGG1 has been identified in eukaryotes, and in particular human brain (hOGG1). hOGG1 has been cloned and shares 50% homology with mouse 8-oxoguanine glycosylase (mOGG1) (4,13). In the present report, the role of the brain's DNA response to RB focused on the activity and regulation of the mammalian base excision repair enzyme OGG1.

In addition to the enzymatic assay, the expression of OGG1 protein was measured by Western immunobloting. However, the detection of a second band with molecular weight essentially different from mOGG1 required more careful characterization. Separation of DNA glycosylases with native PAGE followed by assays of incision activity in various portions of gel disclosed heterogeneity of enzyme activity. Thus, enzymatic incision activity of tested extracts from mouse brain was comprised of two distinct isoforms of OGG1.

A detailed characterization of the isoforms of DNA glycosylase was performed by enzymatic kinetic analysis. Calculation of kinetic constants showed that RB treatment caused an increase in catalytic efficacy in both isoforms of OGG1. The response to RB-induced oxidative DNA damage was to enhance OGG1 catalytic activity (V_{max}/K_m) by a factor of 1.74. RB also increased affinity of OGG1 for the substrate that was demonstrated by decrease in magnitudes of the Michaelis-Menten constant (K_m).

The augmentation of SOD activities in all brain regions and the increased affinity and catalytic activity of OGG1 elicited by RB treatment maintained 8-oxodG levels equal to, or below, the levels found in control animals. In the hippocampus, the levels of oxidative DNA damage following RB treatment was 2.7-fold less than that found in control mice. A similar phenomenon in mouse brain has been reported following treatment with the pro-oxidant diethylmaleate (DEM) (2). A single treatment with DEM elicited a significant increase in the activity of OGG1 in three brain regions with low basal levels of activity. There was no change in the activity of OGG1 in those regions with high basal levels of activity (HP, CP, and MB). This protective response elicited by pro-oxidants such as DEM and RB demonstrate efficient homeostatic mechanisms that maintain a healthy redox status in brain tissues.

The capacity to regulate OGG1 may be important for maintaining genomic integrity in the face of oxidative stress, but endogenous antioxidant defenses also played a role in the brain's response to RB. In fact, the magnitude of the increases in SOD activity across all regions of the brain was greater than the observed increases in OGG1 activity. There was a correlation between OGG1 and SOD activities in different regions of the brain, suggesting that both enzymes may be regulated by a common signal triggered by oxidative stress.

The mechanisms underlying the vulnerability of the brain to different neurotoxicants are complex, but we hypothesize that the capacity to regulate and repair oxidative DNA damage, and to modulate endogenous antioxidant enzymes, are important determinants of a brain region's susceptibility to RB. In the present study, which focused on a single time point 24 h after injection with RB, it was not the intent to determine the earliest signals for triggering and amplifying SOD and OGG1 activities. We imposed the limitation of a single time point for this study to focus on the differential response across brain regions. The robust antioxidant response and enhanced OGG1 catalytic activity in some regions resulted in much lower levels of oxidized base in those brain regions, providing a clue as to the selective vulnerability of specific neuronal populations located in those regions.

The data presented here clearly raise many questions that drive ongoing and future investigations. To further characterize the regulation of OGG1 in response to RB and similar neurotoxicants, it will be important to discover whether the earliest changes in SOD and OGG1 activity (3–6 h after exposure) are due to modification in catalytic activities of the protein and to what extent the response requires up-regulation of SOD and OGG1 mRNA and protein expression. Just as importantly, the effects of RB on viability of specific populations of neurons (e.g., dopaminergic neurons, striatal neurons) in the specific brain regions will need to be investigated and correlated with measures of oxidative DNA damage and

repair. Finally, studies with graded doses of RB will determine whether RB can produce a rigid-akinetic parkinsonian syndrome similar to that produced by other mitochondrial toxicants such as rotenone.

ACKNOWLEDGMENT

This study was supported by VA Merit Grant and DOD grant USAMRMC 03281031.

REFERENCES

1. Bennett, J. W.; Klich, M. Mycotoxins. Clin. Microbiol. Rev. 16:497–516; 2003.
2. Cardozo-Pelaez, F.; Stedeford, T. J.; Brooks, P. J.; Song, S.; Sanchez-Ramos, J. R. Effects of diethylmaleate on DNA damage and repair in the mouse brain. Free Radic. Biol. Med. 33:292–298; 2002.
3. Cascio, C.; Guarneri, R.; Russo, D.; De Leo, G.; Guarneri, M.; Piccoli, F.; Guarneri, P. Pregnenolone sulfate, a naturally occurring excitotoxin involved in delayed retinal cell death. J. Neurochem. 74(6):2380–2391; 2000.
4. Dianov, G.; Bischoff, C.; Piotrowski, J.; Bohr, V. A. Repair pathways for processing of 8-oxoguanine in DNA by mammalian cell extracts. J. Biol. Chem. 273: 33811–33816; 1998.
5. Elstner, E. F.; Heupel, A. Inhibition of nitrite formation from hydroxylammoniumchloride: A simple assay for superoxide dismutase. Anal. Biochem. 70:616–620; 1976.
6. Engelhardt, J. A.; Carlton, W. W.; Carlson, G. P.; Hayes, A. W. Reduction of hepatic and renal nonprotein sulfhydryl content and increased toxicity of rubratoxin B in the Syrian hamster and Mongolian gerbil. Toxicol. Appl. Pharmacol. 96:85–92; 1988.
7. Haley, R. W. Excess incidence of ALS in young Gulf War veterans. Neurology 61:750–756; 2003.
8. Hasegawa, E.; Takeshige, K.; Oishi, T. MPP+ induces NADH-dependent superoxide formation and enhances NADH-dependent lipid peroxidation in bovine heart submitochondrial particles. Biochem. Biophys. Res. Commun. 170:1049–1055; 1990.
9. Hayes, A. W. Action of rubratoxin B on mouse liver mitochondria. Toxicology 6:253–561; 1976.
10. Hood, R. D.; Innes, J. E.; Hayes, A. W. Effects of rubratoxin B on prenatal development in mice. Bull. Environ. Contam. Toxicol. 10:200–207; 1973.
11. Hood, R. D. Effects of concurrent prenatal exposure to rubratoxin B and T-2 toxin in the mouse. Drug Chem. Toxicol. 9:185–190; 1986.
12. Koshakji, R. P.; Wilson, B. J.; Harbison, R. D. Effect of rubratoxin B on prenatal growth and development in mice. Res. Commun. Chem. Pathol. Pharmacol. 5: 584–592; 1973.
13. Krokan, H. E.; Standal, R.; Slupphaug, G. DNA glycosylases in the base excision repair of DNA. Biochem. J. 325:1–16; 1997.
14. Nagashima, H.; Goto, T. Rubratoxin B induces apoptosis in HL-60 cells in the presence of internucleosomal fragmentation. Mycotoxins 46:17–22; 1998.
15. Nagashima, H.; Ishizaki, Y.; Nishida, M.; Morita, I.; Murota, S.; Goto T. Rubratoxin B induces apoptosis in p53-null cells. Mycotoxins 46:35–37; 1998.
16. Nagashima, H.; Nishida, M.; Ishizaki, Y.; Morita, I.; Murota, S.; Goto, T. Cytological effects of rubratoxin B: Morphological change and gap junctional intercellular communication. In: Funatsu, K.; Shirai, Y.; Matsushita, T., eds. Animal cell technology: Basis & applied aspects, vol. 8. Dordrecht: Kluwer Academic Publishers; 1997:571–575.
17. Natori, S.; Sakaki, S.; Kurata, H.; Udagawa, S. I.; Ichinoe, M. Production of rubratoxin B by *Penicillium purpurogenum* Stoll. Appl. Microbiol. 19:613–617; 1970.
18. Phillips, T. D.; Hayes, A. W.; Ho, I. K.; Desaiah, D. Effects of rubratoxin B on the kinetics of cationic and substrate activation of (Na+,K+)-ATPase and p-nitrophenyl phosphatase. J. Biol. Chem. 253:3487–3493; 1978.
19. Siraj, M. Y.; Hayes, A. W. Inhibition of the hepatic cytochrome P-450-dependent monooxygenase system by rubratoxin B in male mice. Toxicol. Appl. Pharmacol. 48:351–359; 1979.
20. Smith, P. K.; Krohn, R. I.; Hermanson, G. T.; Mallia, A. K.; Gartner, F. H.; Provenzano, M. D.; Fujimoto, E. K.; Goeke, N. M.; Olson, B. J.; Klenk, D. C. Measurement of protein using bicinchoninic acid. Anal. Biochem. 150:76–85; 1985.
21. Watson, S. A.; Hayes, A. W. Evaluation of possible sites of action of rubratoxin B-induced polyribosomal disaggregation in mouse liver. J. Toxicol. Environ. Health 2(3):639–650; 1997.
22. Wei, Y. H.; Lu, C. Y.; Lin, T. N.; Wei, R. D. Effect of ochratoxin A on rat liver mitochondrial respiration and oxidative phosphorylation. Toxicology 36:119–130; 1985.
23. Zilinskas, R. A. Iraq's biological weapons. The past as future? JAMA 278:418–424; 1997.